

**IDENTIFICATION OF MUSHROOM METABOLITES AS
POTENTIAL INHIBITORS OF SARS-COV-2 NSP16 FOR COVID-19
TREATMENT**

**Project thesis submitted in partial fulfillment of the requirement for the
degree of Bachelor of Technology**

**In
Bioinformatics**

By

BHOOMI SHARMA (181503)

Under the guidance of

Dr. Raj Kumar



May – 2022

**DEPARTMENT OF BIOTECHNOLOGY AND BIOINFORMATICS
JAYPEE UNIVERSITY OF INFORMATION TECHNOLOGY
WAKNAGHAT, SOLAN, HIMCHAL PRADESH – 173234.**

TABLE OF CONTENTS

Chapter no.	topics	Page no.
	Certificate	4
	Declaration	5
	Acknowledgment	6
	List of figures	7
	List of tables	8
	Abstract	9
Chapter-1	Introduction	
Chapter-2	Review of literature	
	2.1 Introduction	
	2.2 Genomic structure of sars-cov-2	
	2.3 Non – structural proteins (Nsps)	
	2.4 Non – structural protein 16 (Nsp16)	
	2.5 Secondary mushroom metabolites	
	2.6 FDA approved drugs against SARS-CoV-2	
Chapter - 3	Material and methods	
	3.1 Pre-docking	
	3.2 Secondary mushroom metabolites library	
	3.3 Protein preparation and grid preparation for mushroom metabolites	
Chapter - 4	Results and discussion	
	4.1 Virtual screening of the drugs against Nsp16 pre-docking results	
	4.1.1 Selection of top leads from drugs	
	4.2 Virtual screening of mushroom metabolites against Nsp16	
	4.2.1 Selection of top leads from mushroom metabolites	

4.3 Molecular interaction analysis of top leads from virtual screening of drugs and mushroom metabolites with Nsp16.

Chapter - 5

Conclusion

References



CERTIFICATE

This is to certify that the work titled “**Identification of Mushroom Metabolites as Potential Inhibitors of SARS-CoV-2 Nsp16 for COVID-19 Treatment**”, submitted by “**BHOOMI SHARMA (181503)**” in partial fulfillment for the award of the degree of B. Tech in Biotechnology of Jaypee University of Information Technology, Solan has been carried out under my supervision. This work has not been submitted partially or wholly to any other University or Institute for the award of this or any other degree or diploma.

Dr. Raj Kumar

Assistant Professor (Grade – II)

Department of Biotechnology and Bioinformatics

Jaypee University of Information Technology (JUIT)

Waknaghat, Solan, India - 173234

Date:

CANDIDATE'S DECLARATION

I hereby declare that the work presented in this report entitled “**Identification of Mushroom Metabolites as Potential Inhibitors of SARS-CoV-2 Nsp16 for COVID-19 Treatment**” in partial fulfillment of the requirements for the award of the degree of **Bachelor of Technology in Bioinformatics** submitted in the Department of Biotechnology and Bioinformatics, Jaypee University of Information Technology Waknaghat is an authentic record of my work carried out over a period from August 2021 to May 2022 under the supervision of **Dr. Raj Kumar** (Assistant Professor (Grade – II)) Department of Biotechnology and Bioinformatics.

The matter embodied in the report has not been submitted for the award of any other degree or diploma.

Bhoomi Sharma, 181503

This is to certify that the above statement made by the candidate is true to the best of my knowledge.

Dr. Raj Kumar

Assistant Professor (Grade – II)

Department of Biotechnology and Bioinformatics

Date:

ACKNOWLEDGEMENT

It is indeed a great pleasure to thank all those individuals who have, directly or indirectly, contributed and extended their valuable assistance in the progress and completion of this project.

I thank **Dr. Sudhir Kumar**, Head, of the Department of Biotechnology and Bioinformatics, for providing me the opportunity and facilities to carry out the project and for guiding and motivating me whenever required.

I owe my profound gratitude to my project supervisor **Dr. Raj Kumar**, who took a keen interest and guided me all along in my project work titled — **Identification of mushroom metabolites as Potential Inhibitors of SARS-CoV-2 Nsp16 for COVID-19 Treatment**. He provided all the necessary information for carrying out the project. His timely advice, conscientious scrutiny, and scientific approach taught me to work with precision and accuracy and this entity has been a great help to accomplish successful results. I am thankful to him.

It is my privilege to thank my parents for their constant motivation and encouragement. They were always there to provide an affectionate shoulder at odd times or when unsatisfactory results led to frustrations. I am and will always be indebted to their support and care.

Bhoomi Sharma, 181503

LIST OF FIGURES

Figure no	Subject
Fig 1	The structure of SARS-CoV-2 depicting structural proteins- Spike (S), Membrane (M), Envelope (E) and Nucleocapsid protein (N) along with RNA genome, Capsid and receptor Binding Domain (RBD)
Fig 2	The genomic arrangement of the SARS-CoV-2 showing sequential arrangement of the non-structural, structural and accessory genes of SARS-CoV-2. 5' cap leader, UTR replicase, S (Spike), E (Envelope), M (Membrane), N (Nucleocapsid), 3'UTR poly (A) tail with accessory genes such as 3a, 3d, 6, 7a,7b, 8, 9b, 14, and 10 interspersed among the structural genes preceding 3' end of the viral RNA genome.
Fig 3	3D crystal structure of Nsp 10 (Brown) - Nsp16 (Green) methyltransferase complex
Fig 4	2D diagram of Ritonavir
Fig 5	2D diagram of Remdesivir
Fig 6	2D Diagram of Nirmatrelvir
Fig 7	2D diagram of Inotodiol
Fig 8	2D diagram of Neosarcodonin A
Fig 9	2D diagram of Cyathatriol
Fig 10	2D diagram of Cyathin-B3
Fig 11	2D diagram of Erinacine A
Fig 12	2D diagram of Lucidadiol
Fig 13	2D diagram of Enokipodin D
Fig 14	2D diagram of Ganodermediol
Fig 15	2D diagram of Sarcodonin A
Fig 16	2D diagram of Coprinol
Fig 17	Nsp16 protein extracted from 6yz1 protein after removing water and other residues.
Fig 18	Nsp16 protein after minimization and ligand removal

Fig 19	Sinefungin as co-crystal of Nsp16 from 6yz1 protein.
Fig 20	Nsp16 as a macromolecule (Blue) with one of docked ligand
Fig 21	Ritonavir docked with nsp16 protein.
Fig 22	Lucidadiol (left) and Erinacine (right) A docked with nsp16 protein
Fig 23	2D diagrams of molecular interactions of Lucidadiol (Cyan (top)), Ritonavir (Dark Blue (middle)) and Erinacine A (Purple (bottom)).
Fig 24	3D diagrams of molecular interactions of Lucidadiol (Cyan (top)), Ritonavir (Dark Blue (middle)) and Erinacine A (Purple (bottom)).
Fig 25	3D diagram of H-bond interaction of Lucidadiol (Cyan (top)), Ritonavir (Dark Blue (middle)) and Erinacine A (Purple (bottom)).

LIST OF TABLES

Table no.	Subject
Table 1	A brief table about each of the 16 non-structural proteins including their proteins, range, length of each non-structural proteins and their role in the SARS-CoV-2.
Table 2	Docking results of the drugs with the nsp16 macromolecule taken from 6yz1 protein molecule.
Table 3	RMSD calculated for experimental and docking pose step by superimposing co-crystal of 6yz1 protein with the drugs.
Table 4	Docking results of the secondary mushroom metabolites with the Nsp16 macromolecule taken from 6yz1 protein molecule.

ABSTRACT

It has been about three years since the world witnessed the emergence of the highly pathogenic coronavirus disease and caused a pandemic that has affected millions of people's lives. It's past time to put this pandemic behind us and move on to a future free of SARS-CoV-2. To manage the illness and its spread, the development of a safe and effective antiviral is critical. Non-structural viral proteins are a promising target for therapeutic development. Non-structural protein 16 (Nsp16) has proven to be one of the most essential non-structural proteins in the SARS-CoV-2 genome as it plays a vital role in the replication process of the coronavirus. 2'-O-RNA methyltransferase (MTase) is one of the enzymes of this virus that is a potential target for antiviral therapy as it is crucial for RNA cap formation; an essential process for viral RNA stability.

Medicinal fungi have several secondary metabolites, which are an important and diversified chemical space of natural goods. For millennia, medicinal fungi have been used to cure human illnesses in traditional medicine. Here, I have selected 10 secondary mushroom metabolites that have been virtually screened with nsp16 macromolecule to find a therapeutic target against SARS-CoV-2. The FDA approved drugs - Remdesivir, Ritonavir and Nirmatrelvir – were chosen as reference inhibitors for the present study. The binding affinity of reference inhibitors - Remdesivir, Ritonavir and Nirmatrelvir were -7.0 kcal/mol, -7.1 kcal/mol and -6.7 kcal/mol respectively. Further mushroom metabolites – Lucidadiol and Erinacine A exhibited lower binding affinities -7.4 kcal/mol and -7.3 kcal/mol respectively and better molecular interactions than the known reference inhibitors.

Therefore, I propose that the mushroom metabolite Lucidadiol is a potential inhibitor of SARS-CoV-2 Nsp16 and may be considered for further pre-clinical studies.

Keywords: SARS-CoV-2, Secondary mushroom metabolites, Virtual screening, Non-structural proteins, Non-structural protein-16.

Chapter 1

Introduction

1.INTRODUCTION

In the current frameset of the Covid-19 pandemic, which has led to a mass trepidation amongst all generations living, we still don't have an antiviral therapy against the virus that has caused death of more than 620 thousand individuals in last two years.

Scientists have come around 4000 mutations in the Spike (S) protein gene alone. There are few mutations known in the receptor-binding motifs (RBMs), which are responsible for the viral entry via its interaction with human angiotensin-converting enzyme-2 (hACE2) receptor of the human host cell, region of the S protein. These mutations occur during replication leading to thousands of mutations to accumulate and continue to emerge giving rise to new variants. With frequent emergence of new variants and the mutations in glycoprotein S, we are leading to the vaccine escape phase. These variations are known to occur in areas such as the receptor-binding domain (RBD). Thus, making it necessary to formulate vaccines and antiviral drugs that can target more than one viral protein [1]. At present, the munitions stockpile of supported medicines for illnesses brought about by these viruses is fairly restricted and along these lines there is a squeezing need for the disclosure and improvement of restorative specialists for treatment of COVID-19 and other coronaviruses diseases [2]. With the SARS-CoV-2 virus known to have mutated several times over the long run, bringing various genetic variations in the number of viral strains throughout the span of the COVID-19 pandemic, a directly acting antiviral agent can provide a foundation and support to the treatment for the disease.

Coronaviruses are important pathogens of animals and human with high zoonotic potential. SARS-CoV encodes the 2'-O-MTase that is composed of the catalytic subunit nsp16 and the stimulatory subunit nsp10 and plays an important role in virus genome replication and evasion from innate immunity. 2'-O-RNA methyltransferase (MTase) is one of the enzymes of this virus that is a potential target for antiviral therapy as it is crucial for RNA cap formation; an essential process for viral RNA stability. This MTase function is associated with the nsp16 protein, which requires a cofactor, nsp10, for its proper activity [3].

Fungi have a lot of secondary metabolites, which are an important and diversified chemical space of natural goods. For millennia, medicinal fungi have been used to cure human illnesses in

traditional medicine. Such ten secondary mushroom metabolites were selected and a library of was prepared. Only those metabolites with medicinal therapeutic properties were observed were chosen. Two metabolites with antiviral properties (Ganodermediol and Lucidadiol), four with anti-allergic properties (Cyathatriol, Neosarcodonin A, Erinacine A, Sarcodonin A) and others with anti-inflammatory properties were chosen.

In this study, I have selected The FDA approved drugs for SARS-CoV-2 - Remdesivir, Ritonavir and Nirmatrelvir as reference compounds and the binding affinity of each compound with nsp16 molecule was observed. Further, the 10 selected mushroom metabolites were then virtually screened with the Nsp16 molecule and the results were analyzed with the reference compounds.

Chapter 2

Review of Literature

2.REVIEW OF LITERATURE

2.1 Introduction

Severe acute respiratory syndrome coronavirus 2 (SARS-CoV-2) is responsible for the coronavirus disease (COVID 19) global pandemic, which has led to more than 52 million confirmed cases and more than 626 thousand deaths in over 200 countries [2]. Severe acute respiratory syndrome coronavirus 2 (SARS-CoV-2) is a RNA virus that belong to subfamily *Coronavirinae* within the family *Coronaviridae* and genus *Betacoronavirus* [4]. There are four genera of coronaviruses - *Alphacoronavirus*, *Betacoronavirus*, *Gammacoronavirus*, and, *Deltacoronavirus*. While *Alpha* and *Betacoronaviruses* are known to infect human and mammals, *Gamma* and *Deltacoronaviruses* are known to infect birds and fish [5]. The major difference known between the four genera is the presence of non-structural protein-1 (Nsp1) in the *Alpha* and *Betacoronaviruses* while *Gamma* and *Deltacoronaviruses* are known to lack the Nsp1 counterpart [5] SARS-CoV-2 is the seventh known coronavirus strain to infect human beings, after 229E-CoV, NL63-CoV, OC43-CoV, HKU1- CoV, MERS-CoV and SARS-CoV strains. While OC43, HKU1, MERS, SARS, and SARS-2 strains of coronavirus belong to genera *Betacoronaviruses*, NL63 and 229E strains belong to the *Alphacoronaviruses* genus [4]. Amongst all the RNA viruses, coronaviruses are known to have the largest genomes. The genome of SARS-CoV-2 has approximately 29,800 bases that encode 4 structural proteins (Spike Glycoprotein (S), envelope protein (E), membrane protein (M), and nucleocapsid phosphorprotein (N)) and 16 non-structural proteins (non-structural protein-1 – Non-structural protein-16), that act as essential factors for the lifecycle of the virus [2]. The SARS-CoV-2 genome contains a total number of 23 open reading frames (ORFs), which possess the responsibility for the production of the Non-structural proteins (Nsps). They are also responsible for the encoding of the structural proteins [1]. In addition to the structural and non-structural proteins, the SARS-CoV-2 also has 9 accessory proteins (Orf3a, Orf3b, Orf6, Orf7a, Orf7b, Orf8, Orf9b, Orf9c, Orf10) encoded to its 3'end. The SARS-CoV-2 genome consists of a 5'-cap and 3'-poly-A tail. The 5'-end of SARS-CoV-2 consist of a frame-shift between two open read frames (Orf1a and Orf1b) that allows the development of two polypeptides which are through proteolysis are processed to produce the 16 non-structural proteins [5].

2.2 Genomic structure of SARS-CoV-2

The genome of SARS-CoV-2 is comprised of a single-stranded positive-sense RNA [6]. The submission of newly sequenced genome of the SARS-CoV-2 was in the NCBI genome database (NC_045512.2) ~29.9 Kb in size [6]. The genetic composition of SARS-CoV-2 is made of 13–15 (12 functional) open reading frames (ORFs) containing ~30,000 nucleotides. 38% of the GC content and 11 protein-coding genes, with 12 expressed proteins are contained by genome. The genetic arrangement of ORFs highly resembles the SARS-CoV and MERS-CoV [7]. The ORFs are arranged as replicase and protease (1a–1b) and major S, E, M, and N proteins, which follow a typical 5'-3' order of appearance, and are considered as major drug/vaccine targets. An important role of viral entry, fusion, and survival in host cells [8] is played by these genes. The genomic composition of the SARS-CoV-2 is sharing about 89% sequence identity with other CoVs. The retrieval of translated sequences of SARS-CoV-2 proteins was done from the GenBank [9]. The encoding of about 7096 residues long polyprotein which consists of many structural and non-structural proteins is done by whole genome of SARS-CoV-2. Two non-structural proteins ORF1a and ORF1ab followed by structural proteins mainly hold the nucleotide content of the viral genome. Polyproteins pp1a and pp1ab are encoded by ORFs 1a and 1b, where the encoding of polyprotein pp1ab is done by the ribosomal frameshift mechanism of the gene 1b. The further processing of these polyproteins is done by virally encoded proteinases and produces 16 proteins, which are well conserved in all CoVs belonging to the same family. MERS-CoV is closely related to the SARS-CoV-2 moreover it carries a larger genome with ~30,119 nucleotides. A 5' cap structure, a poly(A) tail at 3' end, the rep gene containing 16 NSPs which were numbered as nsp1-nsp16 from the 5' end is contained by the genetic makeup of MERS contains. Around 10 kb of the genome at 3' end constitutes 4 structural genes (S, E, M, N) and 5 accessory proteins (ORF3, ORF4a, ORF4b, ORF5, ORF8). Different epidemiological dynamics makes SARS-CoV-2 relatively more infectious in comparison to the SARS-CoV and MERS-CoV. There is a possibility that other mammalian species act as an “intermediate” or “amplifying” hosts and subsequent ecological separation acquired some or all of the mutations needed for efficient human transmission [6]. Striking similarities to the BAT-CoV is indicated by the comparative sequence analysis of the SARS-CoV-2 genome, in turn suggesting a possible mammalian origin from bats in the Wuhan city of China [6]. Bats are suggested as the natural reservoirs of SARS-

like CoVs, including the SARS-CoV-2 [6] by evidence. CoVs needed intermediate hosts before transmitted to humans. Suggestion of a probable Pangolin origin of SARS-CoV-2 is there, based on the significant similarity of the certain gene [6]. There is still no clarity on how the bat CoVs are genetically transformed and reached to humans. Evidences have suggested that dogs get infected by SARS-CoV-2 too. It is interesting to note that high sequence identity (13 out of 18) is shared among the angiotensin-converting enzyme (ACE2) of humans and dogs (13 out of 18) and thus there is similarity in the binding to the spike RBD of SARS-CoV-2, suggesting human-to-animal transmission [6]. The invasion of a host cell is the first step in SARS-CoV-2 infection, a process that is controlled by the spike (S) glycoprotein [10]. S protein is a glycosylated type I membrane protein, S1 and S2 are two subunits that are contained by S protein. The S protein exists in a trimeric pre-fusion form that is later cleaved by a host furin protease into the two subunits S1 and S2 [5]. Receptor-binding domain is contained in the (RBD) the N-terminal S1 subunit, which mediated binding to the host cell receptor, namely the angiotensin converting enzyme 2 (ACE2) for both SARS-CoV and SARS-CoV-2 [4]. The disassociation between S1 and S2 is fundamentally triggered by Binding of RBD to ACE2, followed by additional cleavage of the S2 subunit at a second specific site by the host serine protease TMPRSS2 leading to the conformational changes in S2 these changes are responsible for the fusion of viral and host membranes and virus entry [10]. Given its crucial role in host recognition and invasion, the S protein has become a major target for the design of drugs and vaccine. The structure of the S protein in various states (pre-fusion, post-fusion, and/or in complex with ACE2) have been reported since sudden emergence of SARS-CoV-2.

The accessory proteins of coronavirus 2 are less well studied, and their involvement in infection is mostly unknown. Even among coronaviruses that are closely related, accessory proteins show the most variation [5]. Orf10 is only found in SARS-CoV-2, and it is not encoded by the closely related SARS-CoV-1. In the same way, SARS-CoV encodes two Orfs, Orf8a and Orf8b, instead of the single Orf8 observed in SARS-CoV-2 [5]. The role of accessory proteins and the various pathways they regulate could lead to the identification of proteins responsible for differences in infectivity or mortality between SARS-CoV and SARS-CoV-2 viruses. In the betacoronavirus subgenus Sarbecovirus, which comprises SARS-CoV and SARS-CoV-2, Orf3a is highly conserved [5].

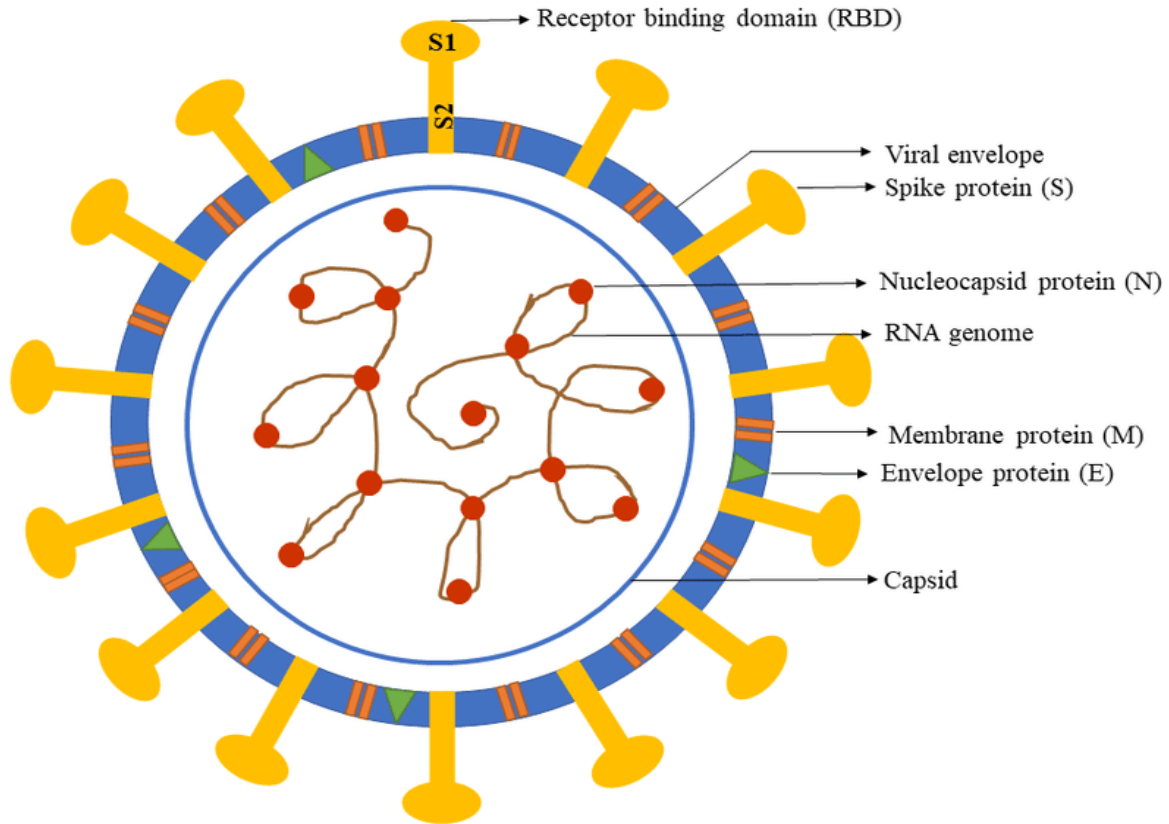


Fig 1: The structure of SARS-CoV-2 depicting structural proteins- Spike (S), Membrane (M), Envelope (E) and Nucleocapsid protein (N) along with RNA genome, Capsid and receptor Binding Domain (RBD) [11]

Orf3a was found to create an ion channel in SARS-CoV, producing a calcium influx and resulting in enhanced DMV formation [5]. In vitro, this pore exhibits a little preference for K^+ and Ca^{2+} over Na^+ , although the ion transported in vivo is unknown. Cryo-EM was used to solve the structure of SARS-CoV-2 Orf3a in its inactive or 'closed' state, revealing that this protein has a new fold, generating a wide and branched channel that connects to the cytoplasm via a huge cavity [5]. Orf3a has been shown to regulate apoptosis, and its pro-apoptotic action in SARS-CoV has been linked to its channel-forming activity [6]. Orf3a can also interact with the structural proteins N, M, and S [5], indicating that it may play a role in virus budding. These findings are in line with the previously described interaction between Orf3a and Nsp3 [5], which is thought to initiate DMV formation. Nsp3 also interacts with Orf9b, implying that the three proteins functions are linked. Despite the information now available, the precise roles of Orf9b

are unknown. It's unclear whether all of Orf9b's contacts are required for its Ubiquitin Ligase activity, or whether Orf9b's interactions with other SARS-CoV-2 proteins imply that it has numerous functions in the virus cycle. The structural characterization of these sub-complexes may provide the knowledge needed to comprehend Orf9b's role [12].

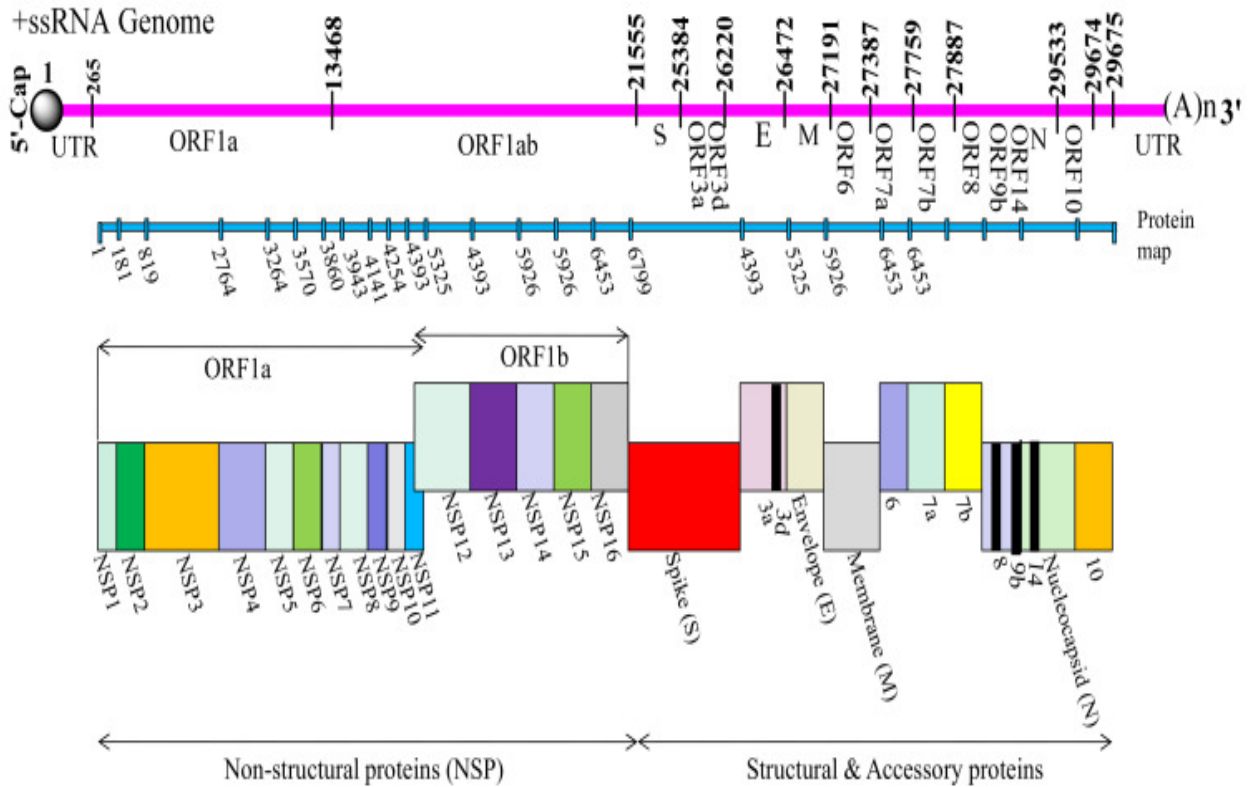


Fig 2: The genomic arrangement of the SARS-CoV-2 showing sequential arrangement of the non-structural, structural and accessory genes of SARS-CoV-2. 5' cap leader, UTR replicase, S (Spike), E (Envelope), M (Membrane), N (Nucleocapsid), 3'UTR poly (A) tail with accessory genes such as 3a, 3d, 6, 7a,7b, 8, 9b, 14, and 10 interspersed among the structural genes preceding 3' end of the viral RNA genome [13].

In addition to the capsid-forming structural proteins, encoding many NSPs that perform numerous roles in the replication and virus assembly processes [6] is done by the viral genome. There is participation of these proteins in viral pathogenesis by modulating early transcription regulation, helicase activity, immunomodulation, gene transactivation, and countering the

antiviral response [6]. Some of the major functions of NSPs in SARS-CoV-2 have been explored by us. The involvement of NSPs of SARS-CoV-2 in many biological processes including, viral genome replication, protein processing, transcription, and proteolysis have been revealed by InterProScan search. There is involvement of these proteins in the RNA-binding, endopeptidase activity, transferase activity, ATP-binding, zinc ion binding, RNA-directed 5'-3' RNA-polymerase activity, exoribonuclease activity, producing 5'-phosphomonoesters, and methyltransferase activity. The retrieval of translated sequence of SARS-CoV-2 ORF1ab polyprotein was done from the GenBank [7] in order to explore the intrinsically unstructured regions in SARS-CoV-2 polyprotein. The intrinsically unstructured regions in SARS-CoV-2 polyprotein through multiple predictors such as PONDR® (Predictor of Natural Disordered Regions), VLXT, VL3, VLS2 [6] and IUPred2A web servers [6] have been predicted by the scientists. These tools have allowed scientists to identify disordered protein regions by predicting the residues which do not possess the tendency to form a structure in the native condition. Residues with a score of >0.5 thresholds were considered to be intrinsically disordered; whereas, residues with a score between 0.2 and 0.5 were considered as flexible. The disordering tendency of each residue in the SARS-CoV-2 polyprotein, where higher values correspond to a higher probability of disorder has been shown by the graph. The SARS-CoV-2 having a chunk of intrinsically disordered regions that lack a well-defined tertiary structure under native conditions have been suggested by the data analysis. All four predictors predicted that the N-terminal region of Nsp3 (920–1020) shows a higher tendency to be disordered. Further, brief insight into the non-structural proteome as well as the unstructured protein regions of the SARS-CoV-2 polyprotein that may be useful to understand the structural basis of infection, structure-based drug discovery and interaction of SARS-CoV-2 proteins with host proteins in different physiological conditions have been provided by this analysis[7].

2.3 Non-structural proteins (Nsps)

NSP (Non-Structural Protein) is a protein which is encoded by a virus which is not a part of the viral particle. The non-structural proteins are involved in impeding inborn immunity and also in inducing virus replication. The Nsps are important parts of the RTC – replication and

transcription complex and immune system evasion. The non-structural proteins help the virus in forming the replication and transcription complex [14].

Nsp 1

Nsp1 intercedes RNA handling and replication [8]. Nsp1 is the N-terminal product of the viral replicase. It is a leader protein host translation inhibitor and mediates RNA replication and processing. Nsp1 is involved in mRNA degradation. Other important activities of nsp1 are adjustment in the cell cycle and biomolecular nuclear-cytoplasmic transport. Upon SARS-CoV-2 disease, NSP1 ties to 18S ribosomal RNA in the mRNA section channel of the ribosome to obstruct the interpretation of mRNA [15].

Nsp2

Nsp2 tweaks the endurance flagging pathway of host cell [8]. Nsp2 is a replicase product essential for proofreading viral replication. It modulates host cell survival signaling pathway by interacting with host PHB1 and PHB2. Other important activities of nsp2 are cell cycle progression, apoptosis and mitochondrial biogenesis [16].

Nsp3

Nsp3 is accepted to isolate the interpreted protein [8]. Nsp3 is a papain-like proteinase contains several domains. It functions as a protease to separate the translated poly-protein into its distinct proteins. Nsp3 is responsible for release of NSP1, NSP2, and NSP3 from the N-terminal region of pp1a and pp1ab. It is the largest protein encoded by the coronaviruses [17].

Nsp4

Nsp4 is a membrane-spanning protein contains trans-membrane domain 2 (TM2). It helps in viral replication-transcription complex and in modification of ER Membranes. It interacts with nsp3 and then host proteins which play an important role in membrane rearrangement in SARS CoV-2 [18].

Nsp5

Nsp5 takes an interest during the time spent polyprotein during replication [8]. Nsp5 is the 3C-like proteinase and main proteinase which plays an important role in the formation of a polyprotein cluster that translates viral RNA and also in the post-translational modification of viral proteins through its ADP ribose phosphatase activity. It cleaves at multiple distinct sites to yield mature and intermediate nonstructural proteins [19].

Nsp6

Nsp6 is putative transmembrane domain protein. It plays a role in the initial induction of autophagosomes from host endoplasmic reticulum. Nsp6 induces formation of ER-derived autophagosomes as well as induces double-membrane vesicles [20].

Nsp7

Nsp7 is an RNA-dependent RNA polymerase. It forms complex with Nsp8 and Nsp12 to yield the RNA polymerase activity of Nsp8. The formation of a hexa-decameric super-complex with Nsp8 adopts a hollow cylinder-like structure implicated replication [21]. The presence of nsp7 and nsp8 fundamentally expands the blend of nsp12 and layout groundwork RNA [8].

Nsp8

Nsp8 is a cofactor of a peptide which makes a heterodimer with the Nsp7. It is a multimeric RNA polymerase and a replicase. It forms a hexa-decameric super-complex with nsp7 that adopts a hollow cylinder-like structure implicated replication. It also forms heterodimer with Nsp7 and Nsp 12. Nsp8 is encoded on the open reading frame ORF1a [21].

Nsp9

Nsp9 is a single-stranded RNA-binding viral protein. It participates in viral replication by acting as an ssRNA-binding protein. It has a diverse form of dimerization that promotes the biological function. NSP8 and NSP9 ties to the 7SL RNA which situates at the Signal Recognition Particle to upset protein dealing to the phone film [8].

Nsp10

Nsp10 is basic for the cap methylation of viral mRNAs [8]. It is a growth-factor-like protein possessing two zinc binding motifs. One site is formed by three cysteine residues (Cys74, Cys77, and Cys90). Another site is formed by four cysteine residues (Cys117, Cys120, Cys128, and Cys130). It functions as a viral transcription by stimulating both nsp14 3'-5' exoribonuclease and nsp16 2'-O-methyltransferase activities. Therefore plays an essential role in viral mRNAs cap methylation [3].

Nsp11

Nsp11 is made of 13 amino acids (SADAQSFLNGFAV) and is identical to the first segment of Nsp12. In the presence of membrane mimetic environment and negatively charged and neutral liposomes, nsp11 remains distorted [22].

Nsp12

Nsp12 contains the RNA-subordinate RNA polymerase (RdRp), a basic Covid replication/record organization [8]. It is a RNA-dependent RNA polymerase (Pol/RdRp). It is responsible for replication and transcription of the viral RNA genome. Nsp12 helps in synthesizing viral DNA and has also been found to suppress a receptor kinase that triggers the retinoic acid-inducible gene and melanoma differentiation-associated protein signaling pathways and that mobilizes interferon beta production [22].

Nsp13

Nsp13 is a zinc-binding domain, NTPase/helicase domain and RNA 5'-triphosphatase. Nsp13 is a helicase core domain that binds ATP while, Zinc-binding domain is involved in replication and transcription. Nsp13 is identified as a good target for anti-virals as it has high sequence conservation and has an essential role in viral replication. Nsp13 ties with ATP and the zinc-restricting area in nsp13 partakes during the time spent replication and record [23].

Nsp14

Nsp14 is a proofreading Exoribonuclease domain (ExoN/nsp14). Nsp14 is known to show exoribonuclease activity acting in a 3' to 5' direction and N⁷-guanine methyltransferase activity.

The exoribonuclease activity is important for the maintenance of the large RNA genome and the methyltransferase activity is important for the stability of the viral RNA [22].

Nsp15

Nsp15 is a EndoRNAse that has two domains: nsp15-A1 and nsp15B-NendoU. Nsp15 has Mn(2+)- dependent endoribonuclease movement [4].

Nsp16

Nsp16 is a 2'-O-methyltransferase (2'-O-Mtase) which forms a part of the replication – transcription complex. Nsp16 has the known function of methyltransferase that mediates mRNA cap 2'-O-ribose methylation to the 5'-cap structure of viral mRNAs. It plays a very important role in immune evasion by mimicking human ACE2 [3].

Name	Protein	Length	Range	Role
NSP1	N-terminal product of the viral replicase	180	1-180	Lead protein that acts as host translation inhibitor and also degrades host mRNAs
NSP2	N-terminal product that is essential for proofreading viral replication	638	181-818	Binds to prohibitin 1 and prohibitin 2 (PHB1 and PHB2)
NSP3	Papain-like proteinase containing several other domains	1945	819-2763	Responsible for release of NSP1, NSP2, and NSP3 from the N-terminal region of pp1a and pp1ab
NSP4	Membrane-spanning protein containing transmembrane domain 2 (TM2)	500	2764-3263	Viral replication transcription complex and it helps modify ER Membranes
NSP5	3C-like proteinase and main proteinase	306	3264-3569	Cleaves at multiple distinct sites to yield mature and intermediate nonstructural proteins
NSP6	Putative transmembrane domain	290	3570-3859	Induces formation of ER-derived autophagosomes. As well as induces double-membrane vesicles

NSP7	RNA-dependent RNA polymerase	83	3860-3942	Forms complex with NSP8 and NSP12 to yield the RNA polymerase activity of NSP8
NSP8	Multimeric RNA polymerase; replicase	198	3943-4140	Makes heterodimer with NSP7 and NSP12
NSP9	A single-stranded RNA-binding viral protein	198	4141-4253	Acts as ssRNA-binding protein in viral replication
NSP10	Growth-factor-like protein possessing two zinc binding motifs	139	4254-4392	Activates the 2'-O-Mtase
NSP11	Consists of 13 amino acids (SADAQSFLNGFAV) and identical to the first segment of Nsp12	13	4393-4405	Unknown
NSP12	RNA-dependent RNA polymerase (Pol/RdRp)	932	4393-5324	Replication and methylation
NSP13	Zinc-binding domain, NTPase/ helicase domain, RNA 5'- triphosphatase	932	5325-5925	A helicase core domain that binds ATP. Zinc-binding domain is involved in replication and transcription
NSP14	Proofreading Exoribonuclease domain (ExoN/nsp14)	527	5926-6452	Exoribonuclease activity acting in a 3'-5' direction and N7-guanine methyltransferase activity
NSP15	EndoRNase; nsp15-A1 and nsp15B-NendoU	346	6453-6798	Mn(2+)-dependent endoribonuclease activity
NSP16	2'-O-ribose methyltransferase	298	6799-7095	Methyltransferase that mediates mRNA cap 2'-O-ribose methylation to the 5'-cap structure of viral mRNAs

Table 1: A brief introduction to each of the 16 non-structural proteins including their range, length of each non-structural proteins and role in the SARS-CoV-2. [13]

2.4 Non-structural protein 16 (Nsp16)

Coronaviruses are known to utilize somewhere in the range of 20 and 30 proteins to complete their viral replication cycle, including disease, invulnerable avoidance, and replication. Among

these, nonstructural protein 16 (Nsp16), a 2'-O-methyltransferase, assumes a fundamental part in resistant avoidance. Nsp16 accomplishes this by mirroring its human homolog, CMTr1, which methylates mRNA to upgrade interpretation effectiveness and recognize self from other. Unlike the human CMTr1, Nsp16 required a limiting accomplice, Nsp10, to initiate its enzymatic action. Thought scientist have figured out the structures of the active Nsp16/Nsp10 complex, structures of inactive, monomeric Nsp16 have yet to be derived. Thus, it is still unclear how Nsp10 activates Nsp16 [9]. There are some NSP-interceded impacts on joining, interpretation, and protein dealing with repressing has guards. Upon SARS-CoV-2 disease, NSP16 ties mRNA acknowledgement areas of the U1 and U2 snRNAs to stifle mRNA grafting. [8].

Most viruses or eukaryotic cell mRNA has the 5'-end covering instrument that assumes an indispensable part in mRNA grafting, interpretation commencement, dependability, and intracellular RNA transport. The capping of the 5'-end happens through a consecutive enzymatic interaction. This includes three chemicals, such as, RNA guanylyltransferase (GTase), RNA triphosphatase (TPase), and RNA guanine-N7-methyltransferase (N7-MTase). This produces a cap-0 construction (m⁷GpppN). It is further methylated at the 2'-O position of mRNA by 2'-O-methyltransferase (2'-O-MTase) and produces the cap-1 (m⁷GpppNm) and cap-2 (m⁷GpppNmNm) structures. This mechanism of mimicking of mRNA capping mechanism helps the virus to avoid the host immune system. MTase and N7-MTase use S-adenosyl-L-methionine (SAM or AdoMet) as a donor of methyl and gives a by-product, S-adenosyl-L-homocysteine (SAH or AdoHcy) [24]. The NSP16 is an m⁷GpppA-specific, SAM-dependent, 2'-O-Mtase and is activated through its binding with the nsp10. Even though with no specific enzymatic activity known and if unique folds, it is known as zinc binding pocket that binds to RNA and stabilizes the SAM binding pocket in the nsp16 to form a stable complex. This nsp10-nsp16-mediated 2'-O-methylation of coronavirus RNA is essential for preventing host recognition and reducing immune response during the time of translation of viral RNA [14]. The presence of nsp10 in the heterodimer of nsp10/nsp16 2'-O-methyltransferase increases the Van der Waals and electrostatic interactions between SAM and nsp16. Thus, the nsp10 acts as a simulator to form strong bond between SAM and nsp16 [25].

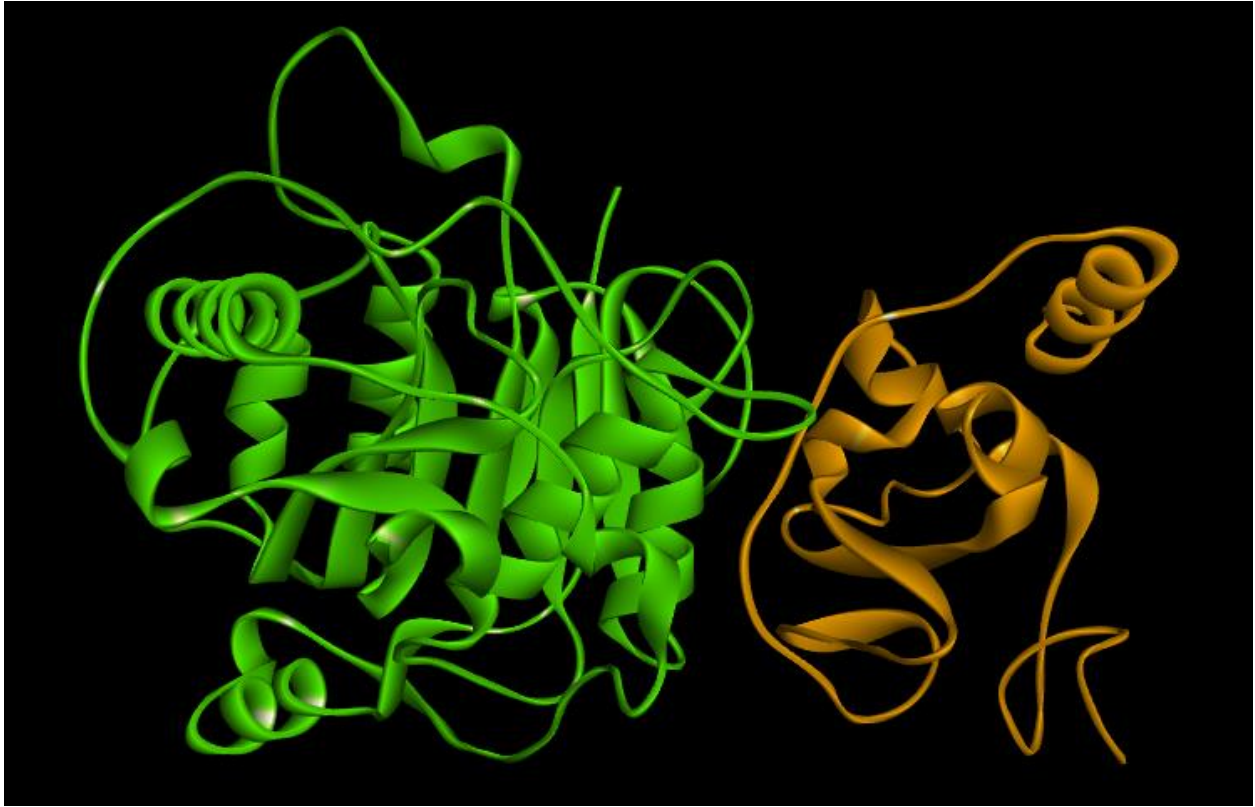


Fig 3: 3D crystal structure of Nsp 10 (Brown) - Nsp16 (Green) methyltransferase complex

2.5 FDA approved drugs against SARS-CoV-2

1. Ritonavir (PubChem CID: 392622)

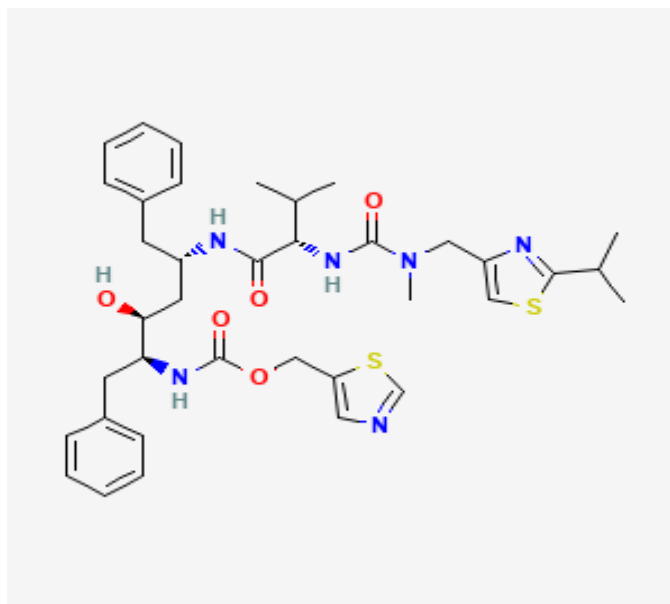


Fig 4: 2D Diagram of Ritonavir

- **Molecular Formula:** C₃₇H₄₈N₆O₅S₂
- **Molecular Weight:** 720.9
- **IUPAC:** 1,3-thiazol-5-ylmethylN-[(2S,3S,5S)-3-hydroxy-5-[[[(2S)-3-methyl-2-[[methyl-[(2-propan-2-yl-1,3-thiazol-4-yl)methyl]carbamoyl]amino]butanoyl]amino]-1,6-diphenylhexan-2-yl]carbamate

Ritonavir is an antiretroviral protease inhibitor that is widely used in combination with other protease inhibitors in the therapy and prevention of human immunodeficiency virus (HIV) infection and the acquired immunodeficiency syndrome (AIDS). Ritonavir can cause transient and usually asymptomatic elevations in serum aminotransferase levels and, rarely, can lead to clinically apparent acute liver injury. In HBV or HCV co-infected patients, highly active antiretroviral therapy with ritonavir may result of an exacerbation of the underlying chronic hepatitis B or C [26].

2. Remdesivir (PubChem CID: 121304016)

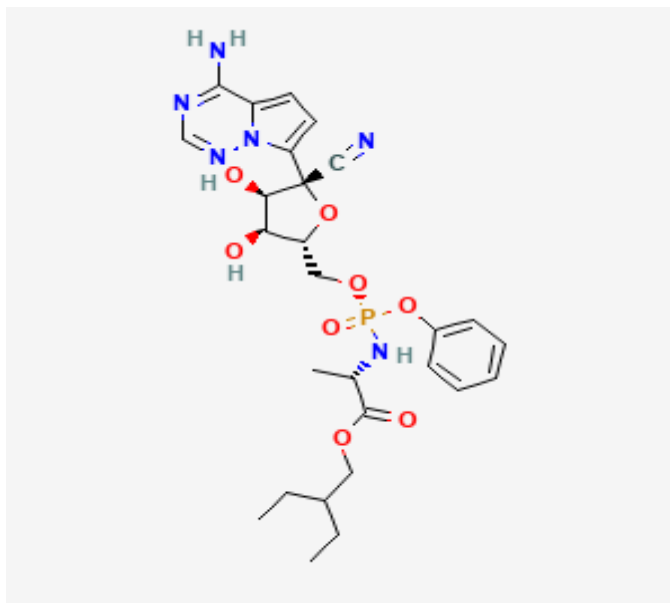


Fig 5: 2D diagram of Remdesivir

- **Molecular Formula:** C₂₇H₃₅N₆O₈P
- **Molecular Weight:** 602.6
- **IUPAC:** 2-ethylbutyl(2S)-2-[[[(2R,3S,4R,5R)-5-(4-aminopyrrolo[2,1-f][1,2,4]triazin-7-yl)-5-cyano-3,4-dihydroxyoxolan-2-yl]methoxy-phenoxyphosphoryl]amino]propanoate

Remdesivir is an antiviral nucleotide analogue used for therapy of severe novel coronavirus disease 2019 (COVID-19) caused by severe acute respiratory syndrome (SARS) coronavirus 2 (CoV-2) infection. Remdesivir therapy is given intravenously for 3 to 10 days and is frequently accompanied by transient, reversible mild-to-moderate elevations in serum aminotransferase levels but has been only rarely linked to instances of clinically apparent liver injury, its hepatic effects being overshadowed by the systemic effects of COVID-19 [27].

3. Nirmatrelvir (PubChem CID: 155903259)

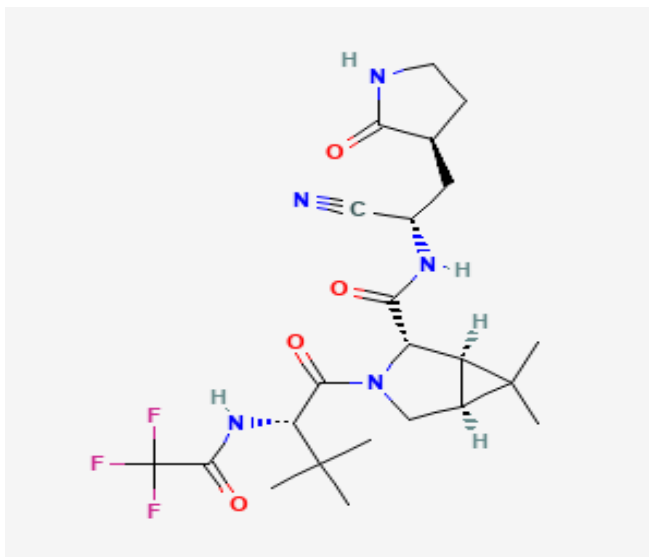


Fig 6: 2D diagram of Nirmatrelvir

- **Molecular Formula:** C₂₃H₃₂F₃N₅O₄
- **Molecular Weight:** 499.0
- **IUPAC:** "(1R,2S,5S)-N-[(1S)-1-cyano-2-[(3S)-2-oxopyrrolidin-3-yl]ethyl]-3-[(2S)-3,3-dimethyl-2-[(2,2,2-trifluoroacetyl)amino]butanoyl]-6,6-dimethyl-3-azabicyclo[3.1.0]hexane-2-carboxamide"

Nirmatrelvir is an orally bioavailable inhibitor of the severe acute respiratory syndrome coronavirus-2 (SARS-CoV-2) 3CL protease (3CLpro), with possible antiviral activity against SARS-CoV-2 and other coronaviruses. On oral administration, nirmatrelvir specifically targets and hinders the activity of SARS-CoV-2 3CLpro. This inhibits the proteolytic cleavage of viral polyproteins, thereby inhibiting the formation of viral proteins including helicase, single-stranded-RNA-binding protein, RNA-dependent RNA polymerase, 20-O-ribose methyltransferase, endoribonuclease and exoribonuclease. This prevents viral transcription and replication. Paxlovid is a co-packaged combination of nirmatrelvir, a second generation protease inhibitor, and ritonavir, a pharmacological enhancer that is used to treated infection with the severe acute respiratory syndrome coronavirus-2 (SARS-CoV-2). Paxlovid is given orally for 5 days in patients early in the course of infection and has not been linked to serum aminotransferase elevations or to clinically apparent liver injury [28].

2.6 Secondary Mushroom Metabolites

1. Inotodiol (PubChem CID: 182264)

Inotodiol is an anti-inflammatory sterol isolated from *Inonotus obliquus* [29].

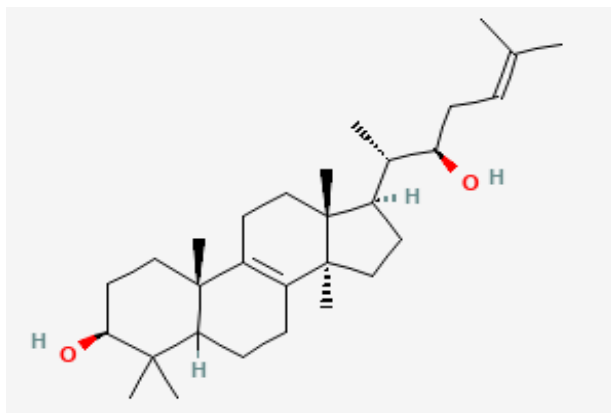


Fig 7: 2D diagram of Inotodiol

- **Molecular Formula:** C₃₀H₅₀O₂
- **IUPAC names:** “(3S,10S,13R,14R,17R)-17-[(2S,3R)-3-hydroxy-6-methylhept-5-en-2-yl]-4,4,10,13,14-pentamethyl-2,3,5,6,7,11,12,15,16,17-decahydro-1H-cyclopenta[a]phenanthren-3-ol”
- **Molecular Weight:** 442.7
- **Hydrogen Bond Donor and Acceptor Count:** 2 and 2
- **Exact Mass:** 442.381080833
- **InChI:** “InChI=1S/C30H50O2/c1-19(2)9-11-24(31)20(3)21-13-17-30(8)23-10-12-25-27(4,5)26(32)15-16-28(25,6)22(23)14-18-29(21,30)7/h9,20-21,24-26,31-32H,10-18H2,1-8H3/t20-,21+,24+,25?,26-,28+,29+,30-/m0/s1”
- **InChI Key:** “KKWJCGCIAHLFNE-UJHWODAZSA-N”
- **Canonical SMILES:**
“CC(C1CCC2(C1(CCC3=C2CCC4C3(CCC(C4(C)C)O)C)C)C)C(CC=C(C)C)O”
- **Isomeric SMILES:**
“C[C@@H]([C@H]1CC[C@@]2([C@@]1(CCC3=C2CCC4[C@@]3(CC[C@@H](C4(C)C)O)C)C)[C@@H](CC=C(C)C)O”

2. Neosarcodonin A (PubChem CID: 101153516)

Neosarcodonin A is an anti-inflammatory cyathane diterpenoids from *Sarcodon scabrosus* and *Hydnellum scabrosum* [30].

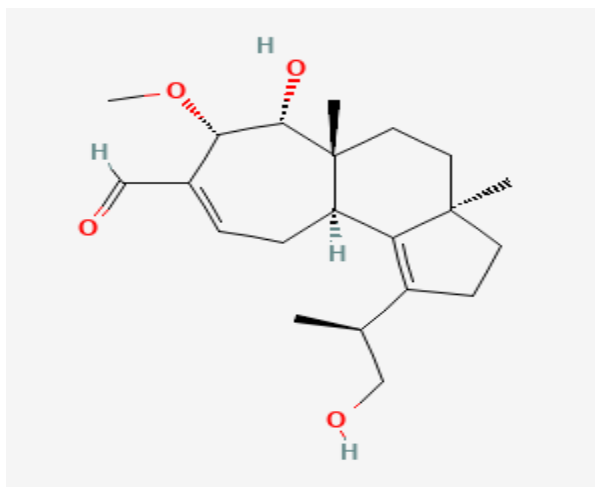


Fig 8: 2D diagram of Neosarcodonin A

- **Molecular Formula:** C₂₁H₃₂O₄
- **IUPAC names:** “(3aR,5aR,6R,7S,10aR)-6-hydroxy-1-[(2S)-1-hydroxypropan-2-yl]-7-methoxy-3a,5a-dimethyl-2,3,4,5,6,7,10,10a-octahydrocyclohepta[e]indene-8-carbaldehyde”
- **Molecular Weight:** 348.5
- **Hydrogen Bond Donor and Acceptor Count:** 2 and 4
- **Exact Mass:** 348.23005950
- **InChI:** “InChI=1S/C21H32O4/c1-13(11-22)15-7-8-20(2)9-10-21(3)16(17(15)20)6-5-14(12-23)18(25-4)19(21)24/h5,12-13,16,18-19,22,24H,6-11H2,1-4H3/t13-,16-,18+,19+,20-,21-/m1/s1”
- **InChI Key:** “KIJQNYNQHIZOJO-MEJVKNBMSA-N”
- **Canonical SMILES:** “CC(CO)C1=C2C3CC=C(C(C(C3(CCC2(CC1)C)C)O)OC)C=O”
- **Isomeric SMILES:**
“C[C@H](CO)C1=C2[C@H]3CC=C([C@@H]([C@@H]([C@@]3(CC[C@]2(C1)C)C)O)OC)C=O”

3. Cyathatriol (PubChem CID: 101316898)

Cyathatriol is an anti-inflammatory and cytotoxic cyathane diterpenoid from *Cyathus africanus* [31].

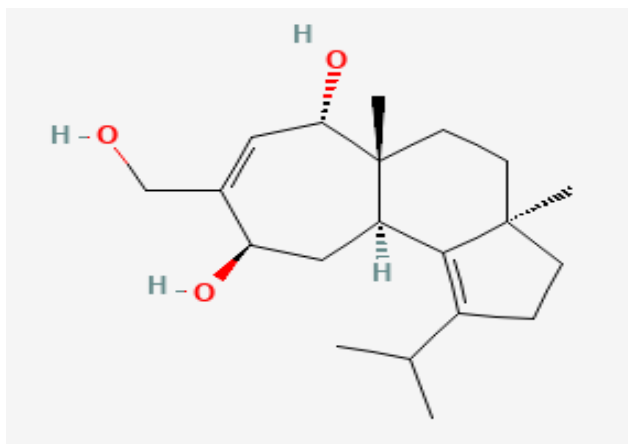


Fig 9: 2D diagram of Cyathatriol

- **Molecular Formula:** C₂₀H₃₂O₃
- **IUPAC names:**
“(3aR,5aR,6S,9R,10aR)-8-(hydroxymethyl)-3a,5a-dimethyl-1-propan-2-yl-2,3,4,5,6,9,10,10a-octahydrocyclohepta[e]indene-6,9-diol”
- **Molecular Weight:** 320.5
- **Hydrogen Bond Donor and Acceptor Count:** 3 and 3
- **Exact Mass:** 320.23514488
- **InChI:**
“InChI=1S/C20H32O3/c1-12(2)14-5-6-19(3)7-8-20(4)15(18(14)19)10-16(22)13(11-21)9-17(20)23/h9,12,15-17,21-23H,5-8,10-11H2,1-4H3/t15-,16-,17+,19-,20-/m1/s1”
- **InChI Key:** “YQGDZWWLYAMTAU-HPUSYDDDSA-N”
- **Canonical SMILES:**
“CC(C)C1=C2C3CC(C(=CC(C3(CCC2(CC1)C)C)O)CO)O”
- **Isomeric SMILES:**
“CC(C)C1=C2[C@H]3C[C@H](C(=C[C@@H]([C@@]3(CC[C@]2(CC1)C)C)O)CO)O”

4. Cyathin-B3 (PubChem CID: 102117112)

Cyathin-B3 is an anti-inflammatory diterpenoid from *Cythus Helenae* [32].

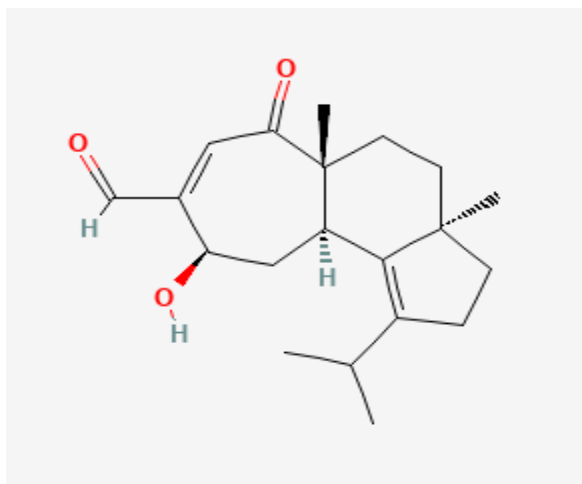


Fig 10: 2D diagram of Cyathin-B3

- **Molecular Formula:** C₂₀H₂₈O₃
- **IUPAC names:** “(3aR,5aR,9R,10aR)-9-hydroxy-3a,5a-dimethyl-6-oxo-1-propan-2-yl-3,4,5,9,10,10a-hexahydro-2H-cyclohepta[e]indene-8-carbaldehyde”
- **Molecular Weight:** 316.4
- **Hydrogen Bond Donor and Acceptor Count:** 1 and 3
- **Exact Mass:** 316.20384475
- **InChI:** “InChI=1S/C20H28O3/c1-12(2)14-5-6-19(3)7-8-20(4)15(18(14)19)10-16(22)13(11-21)9-17(20)23/h9,11-12,15-16,22H,5-8,10H2,1-4H3/t15-,16-,19-,20-/m1/s1”
- **InChI Key:** “HTEKHSBJKOV LAK-XNFNUYLZSA-N”
- **Canonical SMILES:** “CC(C)C1=C2C3CC(C(=CC(=O)C3(CCC2(CC1)C)C)C=O)O”
- **Isomeric SMILES:** “CC(C)C1=C2[C@H]3C[C@H](C(=CC(=O)[C@@]3(CC[C@]2(CC1)C)C)C=O)O”

5. Erinacine A (PubChem CID: 10410568)

Erinacine A is a therapeutic diterpenoid isolated from *Hericium erinaceus* [33].

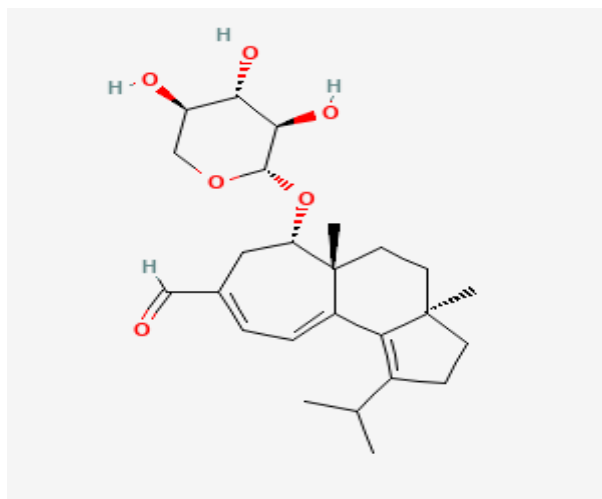


Fig 11: 2D diagram of Erinacine A

- **Molecular Formula:** C₂₅H₃₆O₆
- **IUPAC names:** “(3aR,5aR,6S)-3a,5a-dimethyl-1-propan-2-yl-6-[(2S,3R,4S,5R)-3,4,5-trihydroxyoxan-2-yl]oxy-2,3,4,5,6,7-hexahydrocyclohepta[e]indene-8-carbaldehyde”
- **Molecular Weight:** 432.5
- **Hydrogen Bond Donor and Acceptor Count:** 3 and 6
- **Exact Mass:** 432.25118886
- **InChI:** “InChI=1S/C25H36O6/c1-14(2)16-7-8-24(3)9-10-25(4)17(20(16)24)6-5-15(12-26)11-19(25)31-23-22(29)21(28)18(27)13-30-23/h5-6,12,14,18-19,21-23,27-29H,7-11,13H2,1-4H3/t18-,19+,21+,22-,23+,24-,25-/m1/s1”
- **InChI Key:** “LPPCHLAEVDUIIW-NLLUTMDRSA-N”
- **Canonical SMILES:**
“CC(C)C1=C2C3=CC=C(CC(C3(CCC2(CC1)C)C)OC4C(C(C(CO4)O)O)O)C=O”
- **Isomeric SMILES:**
“CC(C)C1=C2C3=CC=C(C[C@@H]([C@@]3(CC[C@]2(CC1)C)C)O[C@H]4[C@@H]([C@H]([C@@H](CO4)O)O)O)C=O”

6. Lucidadiol (PubChem CID: 10789991)

Lucidadiol is natural product found in *Ganoderma pfeifferii* [34].

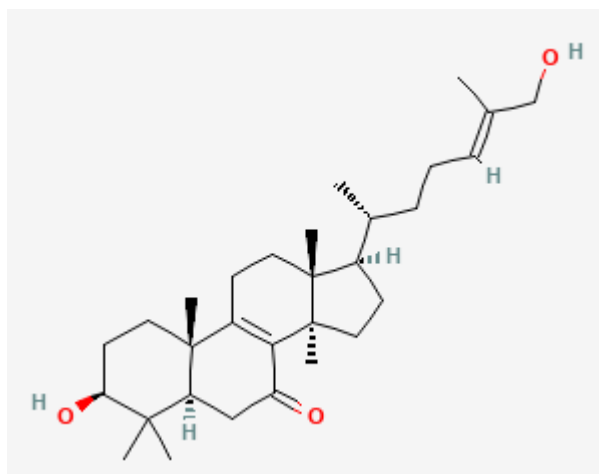


Fig 12: 2D diagram of Lucidadiol

- **Molecular Formula:** C₃₀H₄₈O₃
- **IUPAC names:** “(3*S*,5*R*,10*S*,13*R*,14*R*,17*R*)-3-hydroxy-17-[(*E*,2*R*)-7-hydroxy-6-methylhept-5-en-2-yl]-4,4,10,13,14-pentamethyl-1,2,3,5,6,11,12,15,16,17-decahydrocyclopenta[*a*]phenanthren-7-one”
- **Molecular Weight:** 456.7
- **Hydrogen Bond Donor and Acceptor Count:** 2 and 3
- **Exact Mass:**456.36034359
- **InChI:** ‘InChI = 1S/C30H48O3/c1-19(18-31)9-8-10-20(2)21-11-16-30(7)26-22(12-15-29(21,30)6)28(5)14-13-25(33)27(3,4)24(28)17-23(26)32/h9,20-21,24-25,31,33H,8,10-18H2,1-7H3/b19-9+/t20,-21,-24,+25,+28,-29,-30+/m1/s1’
- **InChI Key:** “AZPOACUDFJKUHI-GPEQXWBKSA-N”
- **Canonical SMILES:**
“CC(CCC=C(C)CO)C1CCC2(C1(CCC3=C2C(=O)CC4C3(CCC(C4(C)C)O)C)C)C”
- **Isomeric SMILES :** “C[C@H]0CC/C=C(\C)/CO”

7. Enokipodin D (PubChem CID: 10901419)

Enokipodin D is a therapeutic diterpenoid found in *Flammulina velutipes* [35].

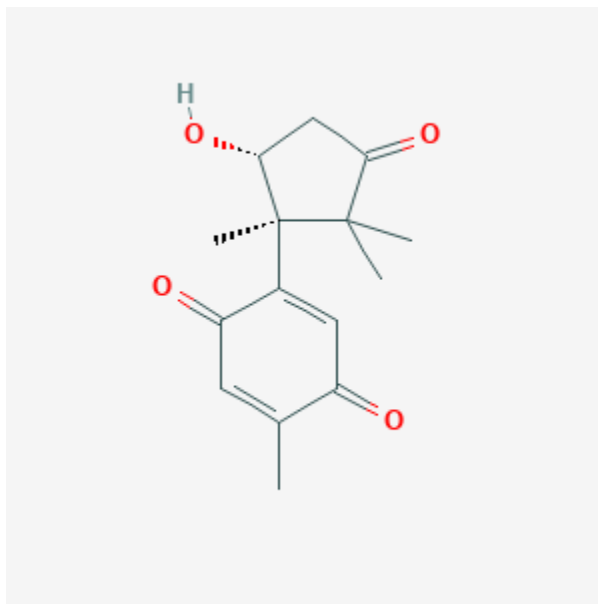


Fig 13: 2D diagram of Enokipodin D

- **Molecular Formula:** C₁₅H₁₈O₄
- **IUPAC names:** “2-[(1S,5R)-5-hydroxy-1,2,2-trimethyl-3-oxocyclopentyl]-5-methylcyclohexa-2,5-diene-1,4-dione”
- **Molecular Weight:** 262.30
- **Hydrogen Bond Donor and Acceptor Count:** 1 and 4
- **Exact Mass:** 262.12050905
- **InChI** : “InChI=1S/C15H18O4/c1-8-5-11(17)9(6-10(8)16)15(4)13(19)7-12(18)14(15,2)3/h5-6,13,19H,7H2,1-4H3/t13-,15+/m1/s1”
- **InChI Key:** “DBTMIHPJDPGOCQ-HIFRSBDPSA-N”
- **Canonical SMILES:** “CC1=CC(=O)C(=CC1=O)C2(C(CC(=O)C2(C)C)O)C”
- **Isomeric SMILES:** “CC1=CC(=O)C(=CC1=O)[C@]2([C@@H](CC(=O)C2(C)C)O)C”

8. Ganodermediol (PubChem CID: 139586903)

Ganodermediol is a sterol isolated from *Ganoderma* [36].

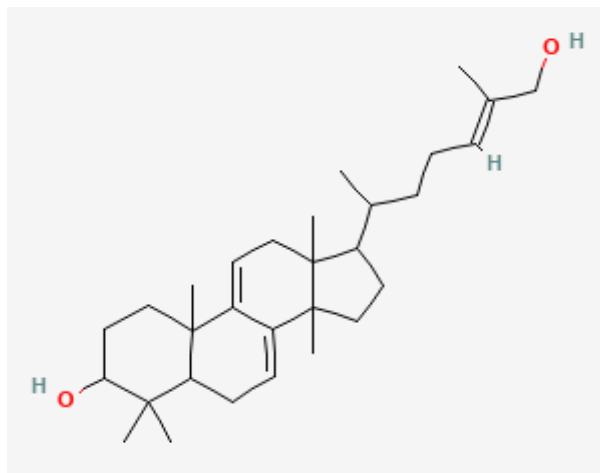


Fig 14: 2d diagram of Ganodermediol

- **Molecular Formula:** C₃₀H₄₈O₂
- **IUPAC names:** “17-[(*E*)-7-hydroxy-6-methylhept-5-en-2-yl]-4,4,10,13,14-pentamethyl-2,3,5,6,12,15,16,17-octahydro-1*H*-cyclopenta[*a*]phenanthren-3-ol”
- **Molecular Weight:** 440.7
- **Hydrogen Bond Donor and Acceptor Count:** 2 and 2
- **Exact Mas:** 440.365430770
- **InChI:** “InChI=1S/C30H48O2/c1-20(19-31)9-8-10-21(2)22-13-17-30(7)24-11-12-25-27(3,4)26(32)15-16-28(25,5)23(24)14-18-29(22,30)6/h9,11,14,21-22,25-26,31-32H,8,10,12-13,15-19H2,1-7H3/b20-9+”
- **InChI Key:** “AOXXVRDKZLRGTJ-AWQFTUOYSA-N”
- **Canonical SMILES:**
“CC(CCC=C(C)CO)C1CCC2(C1(CC=C3C2=CCC4C3(CCC(C4(C)C)O)C)C)C”
- **Isomeric SMILES:**
“CC(CC/C=C(\C)/CO)C1CCC2(C1(CC=C3C2=CCC4C3(CCC(C4(C)C)O)C)C)C”

9. Sarcodonin A (PubChem CID: 17747381)

Sarcodonin A is an anti-viral metabolite found in *Sarcodon Leucopus* [37].

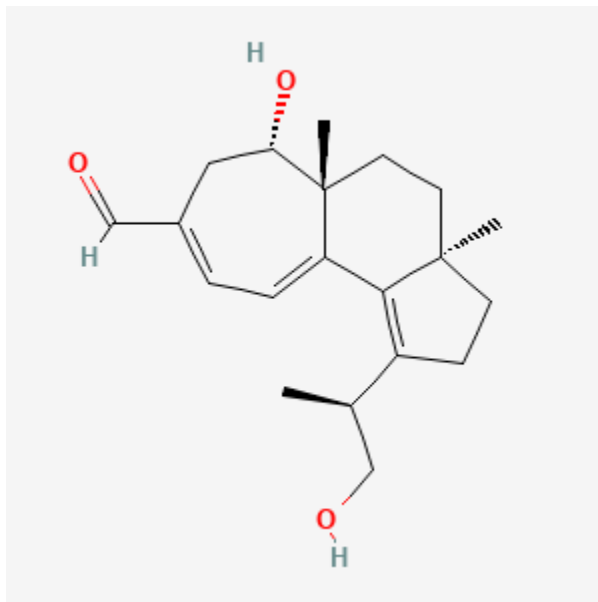


Fig 15: 2D diagram of Sarcodonin A

- **Molecular Formula:** C₂₀H₂₈O₃
- **IUPAC name:** “(3*aR*,5*aR*,6*S*)-6-hydroxy-1-[(2*S*)-1-hydroxypropan-2-yl]-3*a*,5*a*-dimethyl-2,3,4,5,6,7-hexahydrocyclohepta[*e*]indene-8-carbaldehyde”
- **Molecular Weight:** 316.4
- **Hydrogen Bond Donor and Acceptor Count :** 2 and 3
- **Exact Mass:** 316.20384475
- **InChI:** “InChI=1S/C20H28O3/c1-13(11-21)15-6-7-19(2)8-9-20(3)16(18(15)19)5-4-14(12-22)10-17(20)23/h4-5,12-13,17,21,23H,6-11H2,1-3H3/t13-,17+,19-,20-/m1/s1”
- **InChI Key:** “HFBBAANNESGPQZ-ISJOWMGUSA-N”
- **Canonical SMILES:** “CC(CO)C1=C2C3=CC=C(C(C(C3(CCC2(CC1)C)C)O)C=O”
- **Isomeric SMILES :**
“C[C@H](CO)C1=C2C3=CC=C(C[C@@H]([C@@]3(CC[C@]2(CC1)C)C)O)C=O
”

10. Coprinol (PubChem CID: 42608175)

Coprinol is a metabolite found in *Coprinus* and *Coprinopsis cinerea* [38].

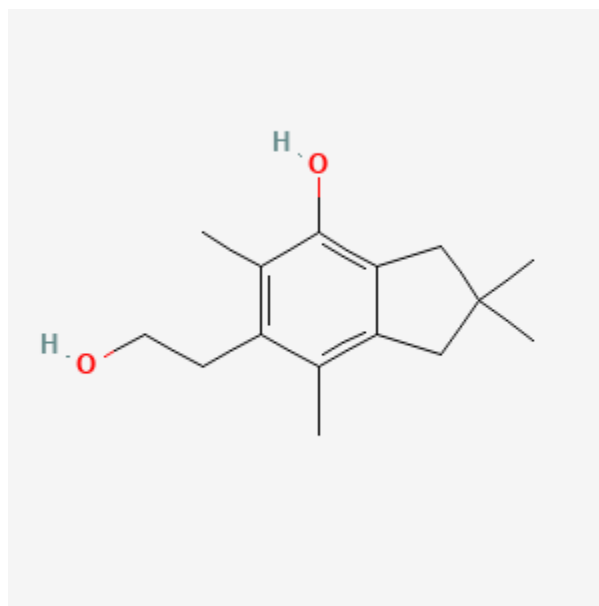


Fig 16: 2D diagram of Coprinol

- **Molecular Formula:** C₁₅H₂₂O₂
- **IUPAC names:** “6-(2-hydroxyethyl)-2,2,5,7-tetramethyl-1,3-dihydroinden-4-ol”
- **Molecular Weight:** 234.33
- **Hydrogen Bond Donor and Acceptor Count :** 2 and 2
- **Exact Mass:** 234.161979940
- **InChI:** InChI=1S/C15H22O2/c1-9-11(5-6-16)10(2)14(17)13-8-15(3,4)7-12(9)13/h16-17H,5-8H2,1-4H3
- **InChI Key:** GCMUHPCLXBXQDH-UHFFFAOYSA-N
- **Canonical SMILES:** CC1=C2CC(CC2=C(C(=C1CCO)C)O)(C)C

Chapter 3

Material and Methods

3.MATERIAL AND METHODS

3.1. Pre-docking

The crystal structure of Nsp16 with PDB ID 6yz1 was downloaded from the RCSB protein data bank. The protein was then prepared for pre-docking and structure based calculations by converting it into. Through this step, residues which were not required for further analysis were highlighted and removed and ligand was obtained.

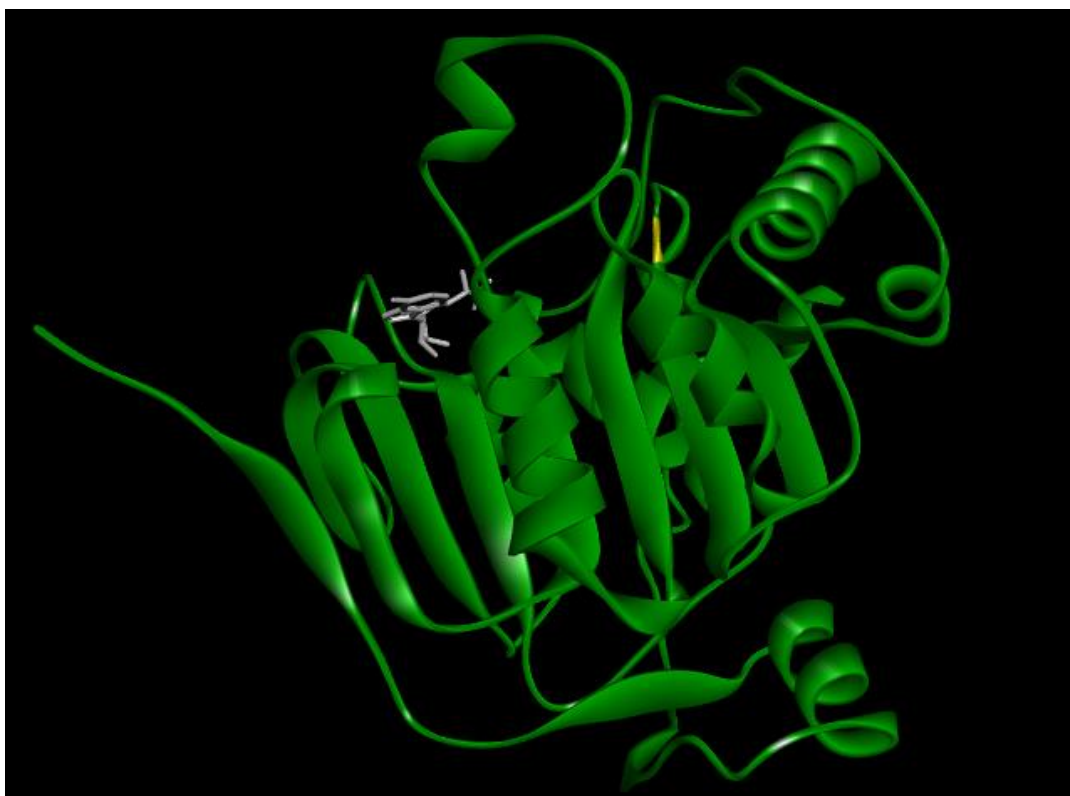


Fig 17: Nsp16 protein extracted from 6yz1 protein after removing water and other residues.

The obtained ligand was further prepared by removing residues and was minimized using Chimera software which helped in addition and minimization of missing loops, removal of crystal waters and protonation of the ligand through its algorithms.

The molecule which was minimized and prepared using Chimera was then loaded on PyRx. The molecule was then selected as a macromolecule and converted into a PDBQT ligand. Through Open Babel tool in PyRx, three drug molecules (ritonavir, remdesivir, nirmatrelvir) were loaded. The drug molecules were then minimized converted and saved into PDBQT ligands.

Using autodock vina wizard, ligand and the three drug molecules were loaded for grid preparation. Exhaustiveness for the docking was set at 8. Coordinates of the grid were set as 22.52 * 21.52 * 22.79

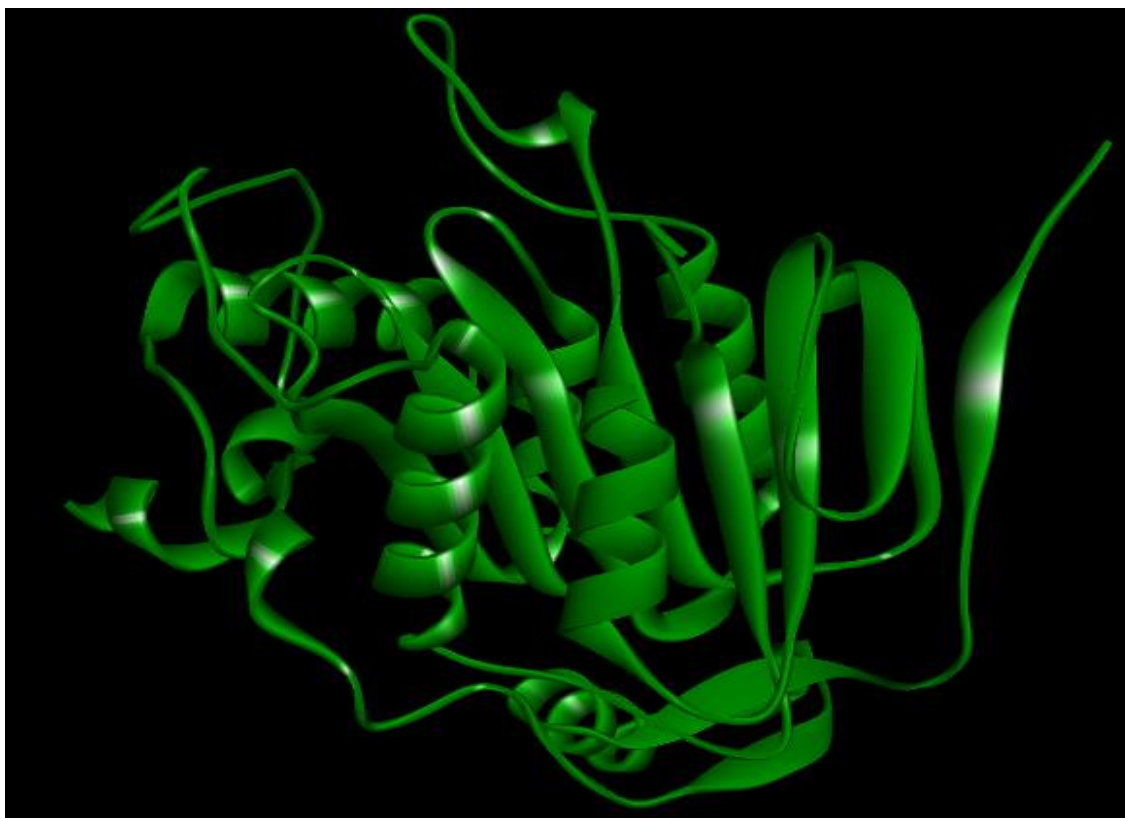


Fig 18: Nsp16 protein after minimization and ligand removal

After the docking of the three drug ligands and the macromolecule, experimental and docking pose were calculated by superimposing co-crystals of the Nsp16 MTase from 6yz1 protein with drug ligands.

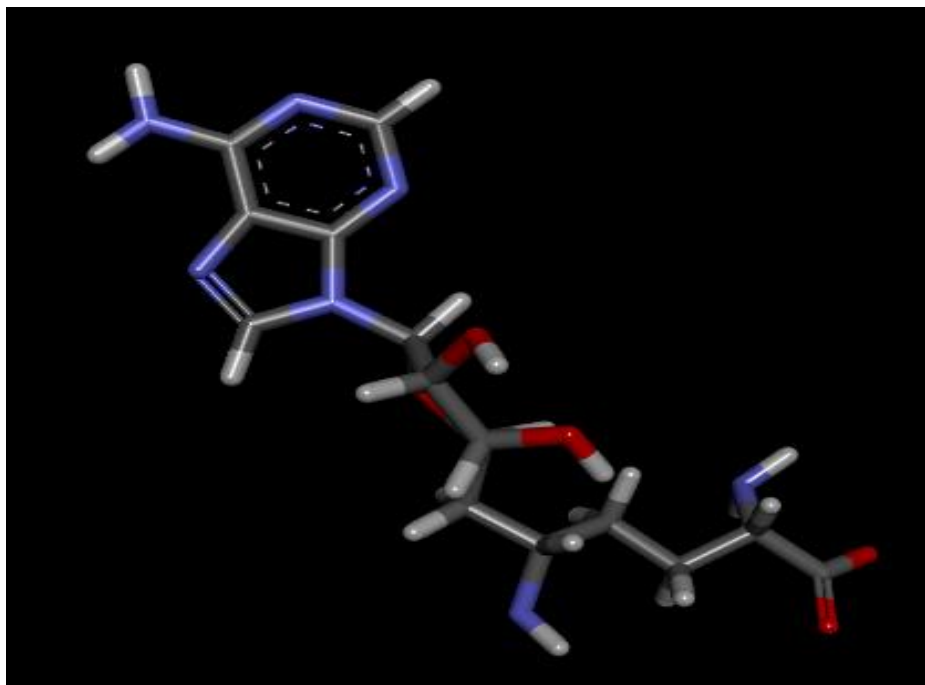


Fig 19: Sinefungin as co-crystal of Nsp16 from 6yz1 protein.

3.2. Secondary mushroom metabolites library

Ten Mushroom metabolites were downloaded from PubChem 3D structures of these secondary metaboloids were saved in SDF and PDBQT file format for further docking procedure. A library of the metabolites was prepared. Only those metabolites were chosen in which medicinal therapeutic properties were seen. Two metabolites with antiviral properties (Ganodermediol and Lucidadiol), four metabolites with anti-allergic properties (Cyathatriol, Neosarcodonin, Erinacine, Sarcodonin), and others with anti-inflammatory properties were chosen.

3.3. Protein preparation and Grid Preparation for Mushroom Metabolites

The crystal structure of Nsp16 MTase from 6yz1 was downloaded from the RCSB protein data bank. The protein was then prepared for docking by converting it into an individual protein molecule. Through this step, residues which were not required for any further analysis were highlighted and removed and ligand was obtained.

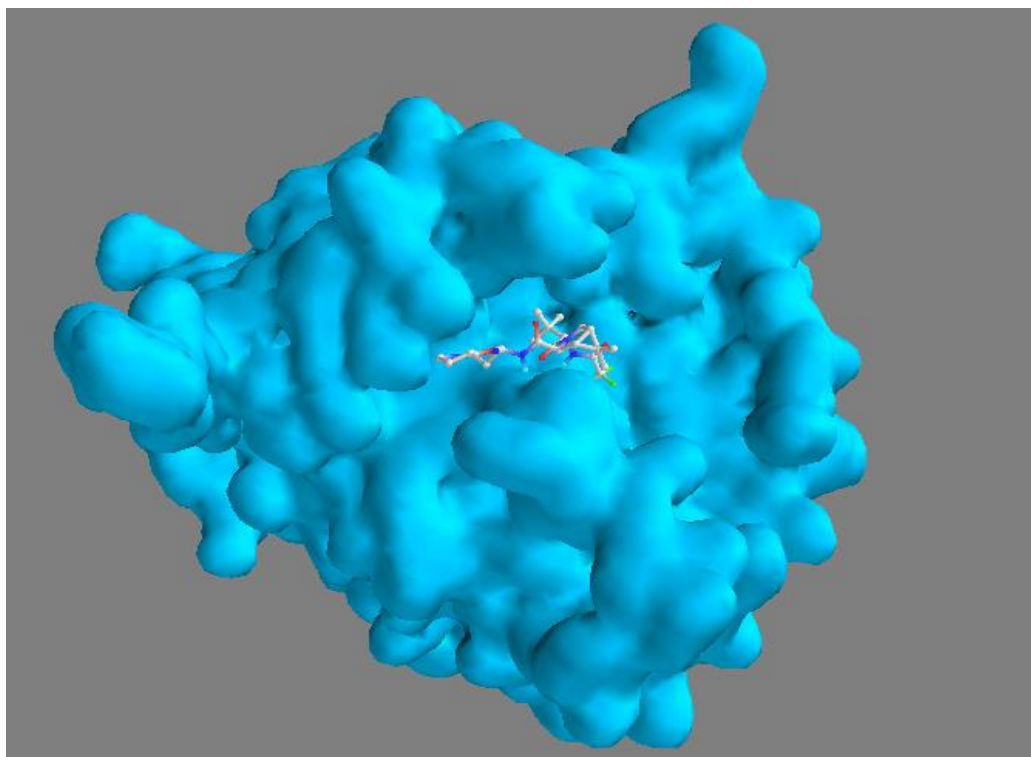


Fig 20: Nsp16 as a macromolecule (Blue) with one of docked ligand

The obtained ligand was further prepared by removing residues and was minimized using Chimera software, which again helped in addition and minimization of missing loops, removal of crystal waters and protonation of ligands through its algorithms.

The molecule which was prepared and minimized using Chimera was then loaded in PyRx. The molecule was selected as a macromolecule and then converted into a PDBQT ligand. Through Open Babel tool in PyRx, ten mushroom metabolites (Inotodiol, Erinacine, Lucidadiol, Enokipodin, Sarcodonin, Coprinol, Neosarcodonin, Cyathatriol, Cyathin, Ganodermediol) were loaded. The metabolites were minimized, converted and then saved as PDBQT ligands.

Using autodock vina wizard, the ligand and the ten secondary mushroom metabolites were loaded for grid preparation. Exhaustiveness for the docking was set at 8 and coordinates of the grid were set as 25 * 24.211 * 24.101.

Chapter 4

Result and Discussion

4. RESULT AND DISCUSSION

4.1. Virtual screening of the drugs against Nsp16 pre-docking results

After the docking of the 6yz1 macromolecule with the three drug ligands the results were as shown in table 2. The grid for the docking was set with the help of active site residues: Gly73, Gy 81, Cys 115 and Tyr 132. The ligand of Ritonavir was noticed to have the lowest binding affinity of -7.6 kcal/mol and a root mean square deviation (RMSD) of 0.0. The three drugs were then superimposed with the co-crystal of 6yz1 to complete experimental and docking pose steps. The concluded root mean square deviation RMSD of all three of the drugs was seen to be ≤ 2.0 Å as shown in the table 3.

Molecules	Binding affinity (kcal/mol)
min_6yz1_ritonavir_3D_uff_E=944.99	-7.1
min_6yz1_remdesivir_uff_E=1212.27	-7.0
min_6yz1_nirmatrelvir_uff_E=1796.64	-6.7

Table 2: Docking results of the drugs with the nsp16 macromolecule taken from 6yz1 protein molecule.

Drugs Ligands	RMSD
Ritonavir	1.30
Nirmatrelvir	1.56
Remdesivir	1.63

Table 3: RMSD calculated for experimental and docking pose step by superimposing co-crystal of 6yz1 protein with the drugs.

4.1.1 Selection of top lead from drugs and nsp16 docking

Since the ligand of Ritonavir was observed with the lowest amount of binding affinity at 7.6 kcal/mol, the compound was chosen as the top lead for further procedure in nsp16 antiviral discovery.

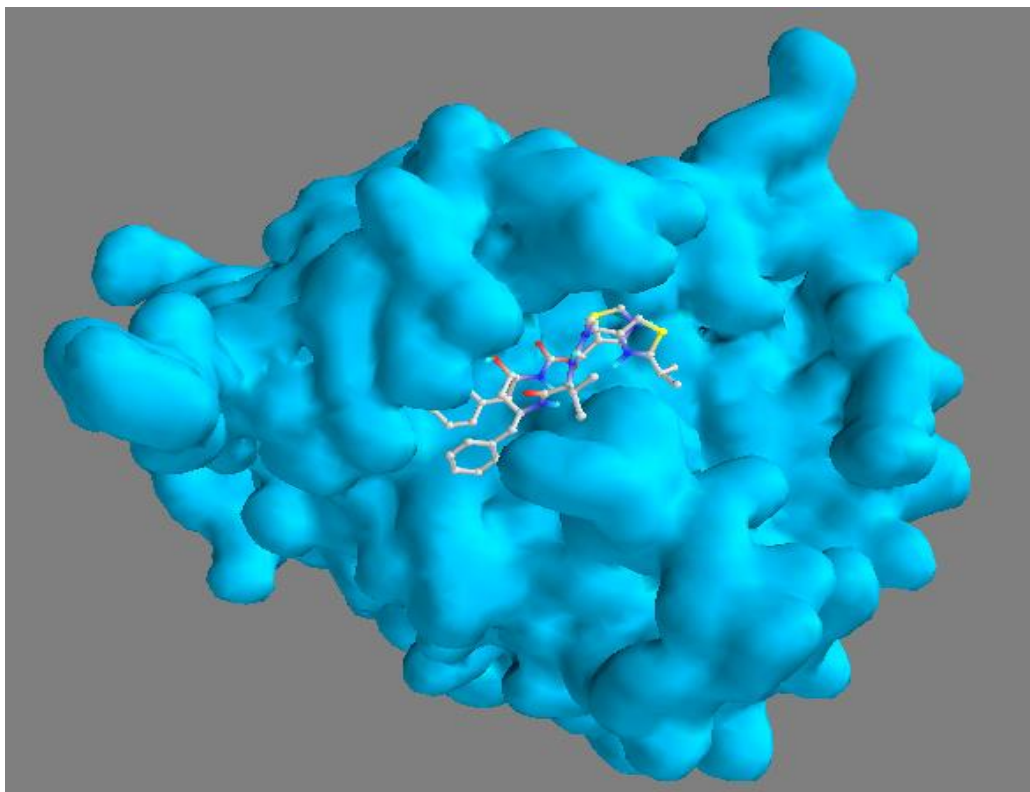


Fig 21: Ritonavir docked with nsp16 protein.

4.2 Virtual Screening of mushroom metabolites against Nsp16

After the affirmation of the experimental and docking pose from the pre-docking results, the virtual screening of the secondary mushroom metabolites was performed. The ligand dataset of 10 compounds was subjected to virtual screening against Nsp16 protein target of COVID-19. The virtual screening was performed using autodock tool implemented in PyRx. The grid for the docking was set with the help of active site residues: Gly73, Gy 81, Cys 115 and Tyr 132.

The results of the virtual screening were obtained in a tabular form as shown in table 4. Compounds of Lucidadiol (PubChem CID: 10789991) and Erinacine-A (PubChem CID: 10410568) were noticed to have binding affinity less than that of the selected drug Ritonavir, which was observed with a binding affinity of -7.6 kcal/mol. The ligand of Lucidadiol was observed with a binding affinity of -7.4 kcal/mol and RMSD of 0.0 while, the ligand of Erinacine-A was observed with a binding affinity of -7.3kcal/mol and RMSD of 0.0.

Mushroom Metabolites Ligands	Binding affinity
min_6yz1_10789991_uff_E=793.63 (Lucidadiol)	-7.4
min_6yz1_10410568_uff_E=723.17 (Erinacine A)	-7.3
min_6yz1_102117112_uff_E=567.60 (Cyathin B3)	-7.0
min_6yz1_139586903_uff_E=792.58 (Ganodemadiol)	-6.7
min_6yz1_182264_uff_E=820.93 (Inotodiol)	-6.7
min_6yz1_42608175_uff_E=331.38 (Coprinol)	-6.3
min_6yz1_101316898_uff_E=491.87 (Cyathatriol)	-5.9
min_6yz1_10901419_uff_E=322.22 (Enokipodin D)	-5.9
min_6yz1_17747381_uff_E=577.02 (Sarcodonin A)	-5.6
min_6yz1_101153516_uff_E=645.31 (Neosarcodonin A)	-5.3

Table 4: Docking results of the secondary mushroom metabolites with the Nsp16 macromolecule taken from 6yz1 protein molecule.

4.2.1 Selection of top lead from mushroom metabolites.

Since the ligand of Lucidadiol and Erinacine A was observed with the lowest amount of binding affinity, the compound was chosen as the top lead for nsp16 antiviral discovery.

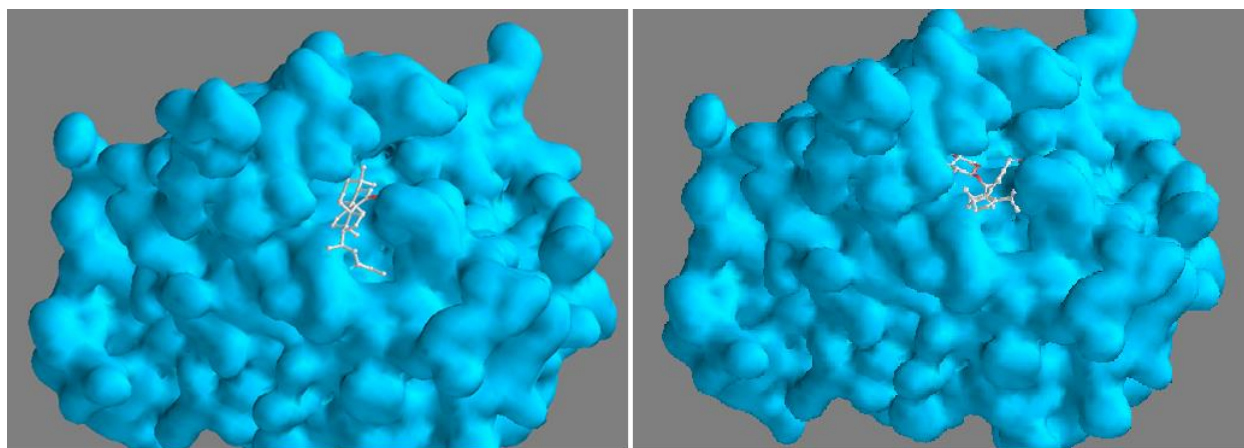


Fig 22: Lucidadiol (left) and Erinacine A (right) docked with nsp16 protein

4.3 Molecular interaction analysis of top leads from Virtual screening of drugs and mushroom metabolites with Nsp16.

The Molecular interactions analysis was performed for the ligands of Ritonavir and Lucidadiol against the macromolecule of Nsp16. The two were then compared and binding site residues Leu 100, Lys 135 and Asp 99 were found common in both the molecular interaction sites as shown in Fig 22 and Fig 23.

For Hydrogen bond interactions, conventional hydrogen bonds were visualized and compared as seen in the results given in the Fig 24.

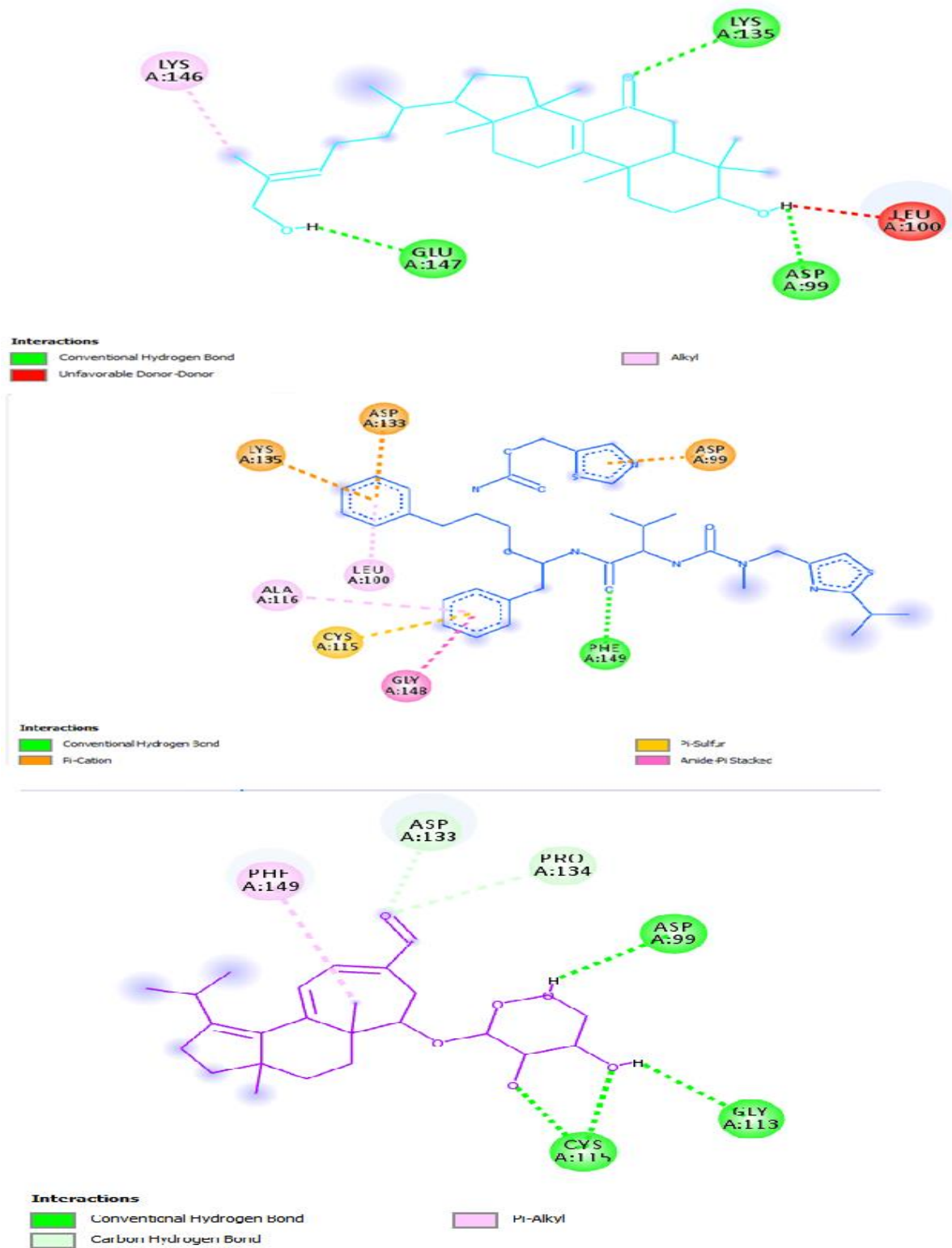


Fig 23: 2D diagrams of molecular interactions of Lucidadiol (Cyan (top)), Ritonavir (Dark Blue (middle)) and Erinacine A (Purple (Bottom)).

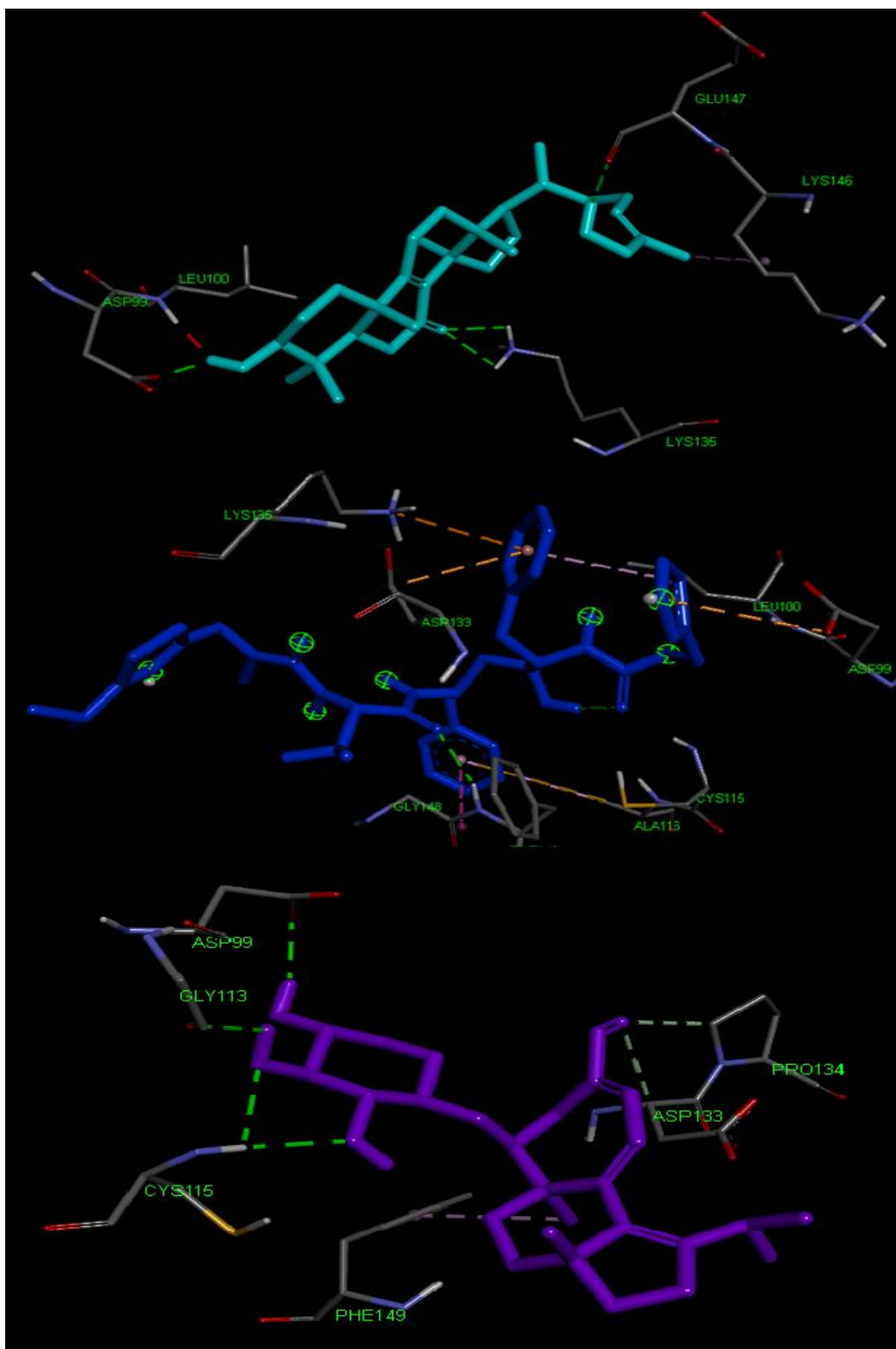


Fig 24: 3D diagram of molecular interactions of Lucidadiol (Cyan (top)), Ritonavir (Dark Blue (middle)) and Erinacine A (Purple(Bottom)).

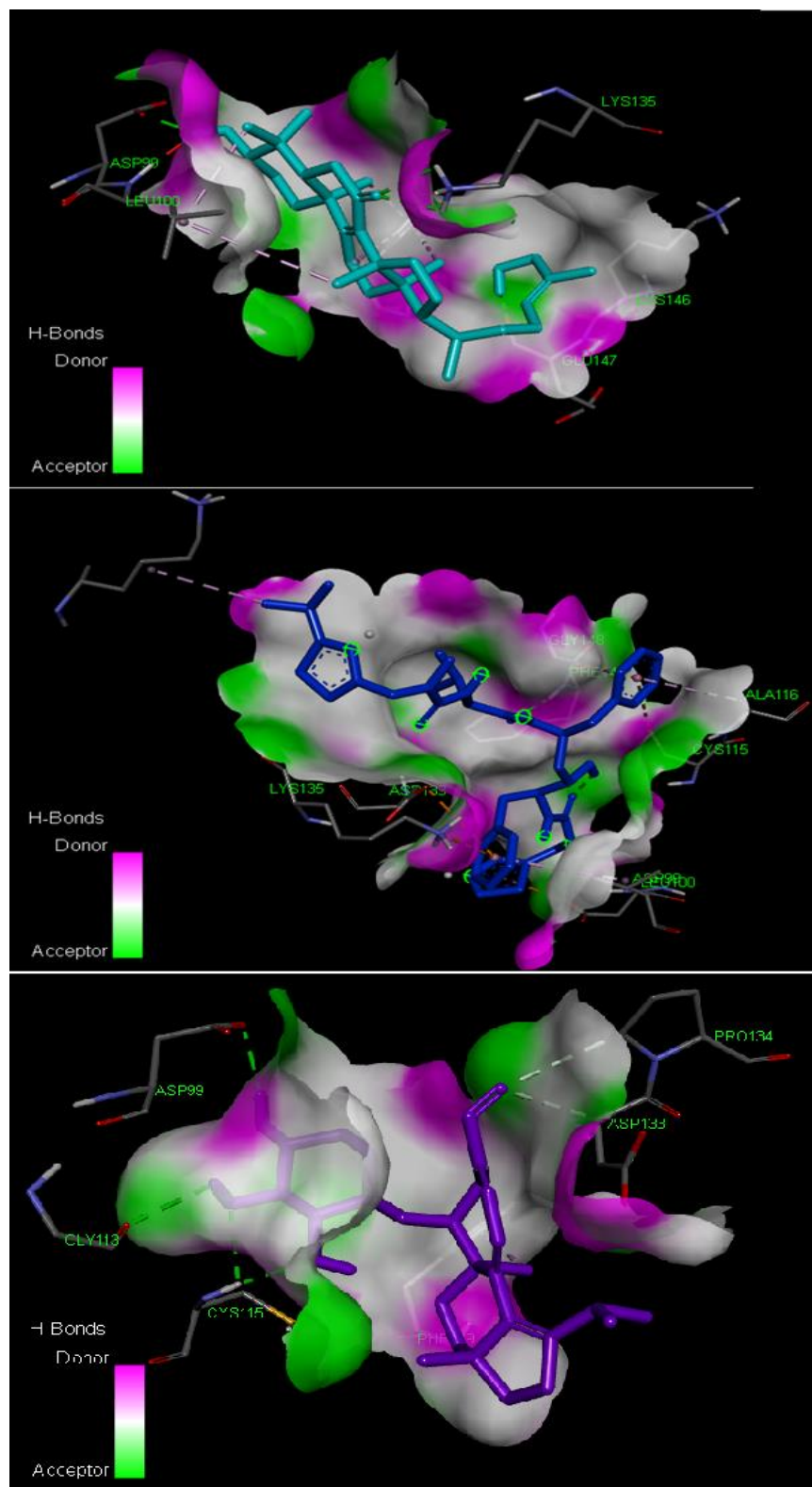


Fig 25: 3D diagram of H-bond interaction of Lucidadiol (Cyan (top)), Ritonavir (Dark Blue (middle)) and Erinacine A (Purple (Bottom)).

Chapter 5

Conclusion

5. CONCLUSION

Through the research and experiments conducted above, it can be concluded that the secondary mushroom metabolite Lucidadiol (PubChem CID: 10789991) that is known to have anti-viral properties and is found a promising therapeutic inhibitor against SARS-CoV-2 targeting specially Nsp16. This could be concluded because Lucidadol was observed to have the lowest binding affinity (-7.4 kcal/mol) amongst the 10 secondary mushroom metabolites that were docked with the Nsp16 macromolecule.

6. REFERENCES

- [1] B. Cosar *et al.*, “SARS-CoV-2 Mutations and their Viral Variants,” *Cytokine & Growth Factor Reviews*, vol. 63, pp. 10–22, Jul. 2021, doi: 10.1016/j.cytogfr.2021.06.001.
- [2] P. Krafcikova, J. Silhan, R. Nencka, and E. Boura, “Structural analysis of the SARS-CoV-2 methyltransferase complex involved in RNA cap creation bound to sinefungin,” *Nature Communications*, vol. 11, no. 1, p. 3717, Jul. 2020, doi: 10.1038/s41467-020-17495-9.
- [3] E. Decroly *et al.*, “Crystal Structure and Functional Analysis of the SARS-Coronavirus RNA Cap 2'-O-Methyltransferase nsp10/nsp16 Complex,” *PLoS Pathogens*, vol. 7, no. 5, p. e1002059, May 2011, doi: 10.1371/journal.ppat.1002059.
- [4] S. Barage *et al.*, “Identification and characterization of novel RdRp and Nsp15 inhibitors for SARS-COV2 using computational approach,” *Journal of Biomolecular Structure and Dynamics*, vol. 40, no. 6, pp. 2557–2574, Nov. 2020, doi: 10.1080/07391102.2020.1841026.
- [5] G. Mariano, R. J. Farthing, S. L. M. Lale-Farjat, and J. R. C. Bergeron, “Structural Characterization of SARS-CoV-2: Where We Are, and Where We Need to Be,” *Frontiers in Molecular Biosciences*, vol. 7, p. 605236, 2020, doi: 10.3389/fmolb.2020.605236.
- [6] A. A. T. Naqvi *et al.*, “Insights into SARS-CoV-2 genome, structure, evolution, pathogenesis and therapies: Structural genomics approach,” *Biochimica et Biophysica Acta. Molecular Basis of Disease*, vol. 1866, no. 10, p. 165878, Oct. 2020, doi: 10.1016/j.bbadis.2020.165878.
- [7] “Severe acute respiratory syndrome coronavirus 2 isolate Wuhan-Hu-1, complete genome,” *NCBI Nucleotide*, Jul. 2020. Available: https://www.ncbi.nlm.nih.gov/nuccore/NC_045512.2
- [8] M.-Y. Wang, R. Zhao, L.-J. Gao, X.-F. Gao, D.-P. Wang, and J.-M. Cao, “SARS-CoV-2: Structure, Biology, and Structure-Based Therapeutics Development,” *Frontiers in Cellular and Infection Microbiology*, vol. 10, no. 587269, Nov. 2020, doi: 10.3389/fcimb.2020.587269.

- [9] M. F. Sk, N. A. Jonniya, R. Roy, S. Poddar, and P. Kar, “Computational Investigation of Structural Dynamics of SARS-CoV-2 Methyltransferase-Stimulatory Factor Heterodimer nsp16/nsp10 Bound to the Cofactor SAM,” *Frontiers in Molecular Biosciences*, vol. 7, Nov. 2020, doi: 10.3389/fmolb.2020.590165.
- [10] M. A. Tortorici and D. Veessler, “Chapter Four - Structural insights into coronavirus entry,” *ScienceDirect*, Jan. 01, 2019. <https://www.sciencedirect.com/science/article/pii/S0065352719300284> (accessed Dec. 13, 2021).
- [11] P. Saini, “COVID-19 pandemic: potential phase III vaccines in development,” *The Applied Biology & Chemistry Journal*, pp. 21–33, Sep. 2020, doi: 10.52679/tabcj.2020.0004.
- [12] N. Vithani *et al.*, “SARS-CoV-2 Nsp16 activation mechanism and a cryptic pocket with pan-coronavirus antiviral potential,” *Biophysical Journal*, vol. 120, no. 14, pp. 2880–2889, Jul. 2021, doi: 10.1016/j.bpj.2021.03.024.
- [13] R. Yadav *et al.*, “Role of Structural and Non-Structural Proteins and Therapeutic Targets of SARS-CoV-2 for COVID-19,” *Cells*, vol. 10, no. 4, p. 821, Apr. 2021, doi: 10.3390/cells10040821.
- [14] P. V’kovski, A. Kratzel, S. Steiner, H. Stalder, and V. Thiel, “Coronavirus biology and replication: implications for SARS-CoV-2,” *Nature Reviews Microbiology*, vol. 19, pp. 155–170, Oct. 2020, doi: 10.1038/s41579-020-00468-6.
- [15] Y.-Q. Min, Q. Mo, J. Wang, F. Deng, H. Wang, and Y.-J. Ning, “SARS-CoV-2 nsp1: Bioinformatics, Potential Structural and Functional Features, and Implications for Drug/Vaccine Designs,” *Frontiers in Microbiology*, vol. 11, Sep. 2020, doi: 10.3389/fmicb.2020.587317.
- [16] C. T. Cornillez-Ty, L. Liao, J. R. Yates, P. Kuhn, and M. J. Buchmeier, “Severe Acute Respiratory Syndrome Coronavirus Nonstructural Protein 2 Interacts with a Host Protein Complex Involved in Mitochondrial Biogenesis and Intracellular Signaling,” *Journal of Virology*, vol. 83, no. 19, pp. 10314–10318, Jul. 2009, doi: 10.1128/jvi.00842-09.

- [17] J. Lei, Y. Kusov, and R. Hilgenfeld, “Nsp3 of coronaviruses: Structures and functions of a large multi-domain protein,” *Antiviral Research*, vol. 149, pp. 58–74, Jan. 2018, doi: 10.1016/j.antiviral.2017.11.001.
- [18] Y. Sakai, K. Kawachi, Y. Terada, H. Omori, Y. Matsuura, and W. Kamitani, “Two-amino acids change in the nsp4 of SARS coronavirus abolishes viral replication,” *Virology*, vol. 510, pp. 165–174, Oct. 2017, doi: 10.1016/j.virol.2017.07.019.
- [19] K. Anand, “Structure of coronavirus main proteinase reveals combination of a chymotrypsin fold with an extra alpha-helical domain,” *The EMBO Journal*, vol. 21, no. 13, pp. 3213–3224, Jul. 2002, doi: 10.1093/emboj/cdf327.
- [20] E. M. Cottam, M. C. Whelband, and T. Wileman, “Coronavirus NSP6 restricts autophagosome expansion,” *Autophagy*, vol. 10, no. 8, pp. 1426–1441, Jun. 2014, doi: 10.4161/auto.29309.
- [21] A. J. W. te Velthuis, S. H. E. van den Worm, and E. J. Snijder, “The SARS-coronavirus nsp7+nsp8 complex is a unique multimeric RNA polymerase capable of both de novo initiation and primer extension,” *Nucleic Acids Research*, vol. 40, no. 4, pp. 1737–1747, Feb. 2012, doi: 10.1093/nar/gkr893.
- [22] L. Subissi *et al.*, “One severe acute respiratory syndrome coronavirus protein complex integrates processive RNA polymerase and exonuclease activities,” *Proceedings of the National Academy of Sciences*, vol. 111, no. 37, pp. E3900–E3909, Sep. 2014, doi: 10.1073/pnas.1323705111.
- [23] K.-J. Jang, S. Jeong, D. Y. Kang, N. Sp, Y. M. Yang, and D.-E. Kim, “A high ATP concentration enhances the cooperative translocation of the SARS coronavirus helicase nsP13 in the unwinding of duplex RNA,” *Scientific Reports*, vol. 10, no. 1, Mar. 2020, doi: 10.1038/s41598-020-61432-1.
- [24] S. Lin *et al.*, “Crystal structure of SARS-CoV-2 nsp10/nsp16 2'-O-methylase and its implication on antiviral drug design,” *Signal Transduction and Targeted Therapy*, vol. 5, no. 1, Jul. 2020, doi: 10.1038/s41392-020-00241-4.

- [25] M. Rosas-Lemus *et al.*, “The crystal structure of nsp10-nsp16 heterodimer from SARS-CoV-2 in complex with S-adenosylmethionine,” *bioRxiv*, p. 2020.04.17.047498, Apr. 2020, doi: 10.1101/2020.04.17.047498.
- [26] PubChem, “Ritonavir,” *pubchem.ncbi.nlm.nih.gov*, Mar. 26, 2005.
<https://pubchem.ncbi.nlm.nih.gov/compound/392622>
- [27] PubChem, “Remdesivir,” *pubchem.ncbi.nlm.nih.gov*, Aug. 06, 2016.
<https://pubchem.ncbi.nlm.nih.gov/compound/Remdesivir>
- [28] PubChem, “Nirmatrelvir,” *pubchem.ncbi.nlm.nih.gov*, May 01, 2021.
<https://pubchem.ncbi.nlm.nih.gov/compound/155903259>
- [29] PubChem, “(3S,10S,13R,14R,17R)-17-[(2S,3R)-3-hydroxy-6-methylhept-5-en-2-yl]-4,4,10,13,14-pentamethyl-2,3,5,6,7,11,12,15,16,17-decahydro-1H-cyclopenta[a]phenanthren-3-ol,” *pubchem.ncbi.nlm.nih.gov*, Aug. 09, 2005.
<https://pubchem.ncbi.nlm.nih.gov/compound/182264>
- [30] PubChem, “Neosarcodonin A,” *pubchem.ncbi.nlm.nih.gov*, Dec. 18, 2015.
<https://pubchem.ncbi.nlm.nih.gov/compound/101153516>
- [31] PubChem, “Cyathin-B3,” *pubchem.ncbi.nlm.nih.gov*, Mar. 06, 2005.
<https://pubchem.ncbi.nlm.nih.gov/compound/102117112>
- [32] PubChem, “Cyathatriol,” *pubchem.ncbi.nlm.nih.gov*, Dec. 18, 2015.
<https://pubchem.ncbi.nlm.nih.gov/compound/101316898>
- [33] PubChem, “Erinacine A,” *pubchem.ncbi.nlm.nih.gov*, Oct. 25, 2006.
<https://pubchem.ncbi.nlm.nih.gov/compound/10410568>
- [34] PubChem, “Lucidadiol,” *pubchem.ncbi.nlm.nih.gov*, Oct. 26, 2006.
<https://pubchem.ncbi.nlm.nih.gov/compound/Lucidadiol>
- [35] PubChem, “Enokipodin D,” *pubchem.ncbi.nlm.nih.gov*, Oct. 26, 2006.
<https://pubchem.ncbi.nlm.nih.gov/compound/10901419>

[36] PubChem, “(3S,5R,10S,13R,14R,17R)-17-[(2R)-7-hydroxy-6-methylhept-5-en-2-yl]-4,4,10,13,14-pentamethyl-2,3,5,6,12,15,16,17-octahydro-1H-cyclopenta[a]phenanthren-3-ol,” *pubchem.ncbi.nlm.nih.gov*, Feb. 08, 2007.
<https://pubchem.ncbi.nlm.nih.gov/compound/139586903>

[37] PubChem, “Sarcodonin A,” *pubchem.ncbi.nlm.nih.gov*, Nov. 14, 2007.
<https://pubchem.ncbi.nlm.nih.gov/compound/17747381>

[38] PubChem, “Coprinol,” *pubchem.ncbi.nlm.nih.gov*, Jun. 10, 2009.
<https://pubchem.ncbi.nlm.nih.gov/compound/42608175>